Imaging Neuroscience
an open access journal

Research Article

Flicker light stimulation induces thalamocortical hyperconnectivity with LGN and higher-order thalamic nuclei

Ioanna A. Amaya[a,b,c], Marianna E. Schmidt[a,d], Marie T. Bartossek[a,e], Johanna Kemmerer[f], Evgeniya Kirilina[g], Till Nierhaus[a], Timo T. Schmidt[a]

[a]Neurocomputation and Neuroimaging Unit, Department of Education and Psychology, Freie Universität Berlin, Berlin, Germany
[b]Charité – Universitätsmedizin Berlin, Einstein Center for Neurosciences Berlin, Berlin, Germany
[c]Berlin School of Mind and Brain, Humboldt-Universität zu Berlin, Berlin, Germany
[d]Max Planck School of Cognition, Leipzig, Germany
[e]Faculty of Psychology, TUD Dresden University of Technology, Dresden, Germany
[f]Department of Psychiatry, Psychotherapy and Psychosomatic Medicine, Vivantes Hospital Am Urban und Vivantes Hospital im Friedrichshain, Charité-Universitätsmedizin Berlin, Berlin, Germany
[g]Department of Neurophysics, Max Planck Institute for Human Cognitive and Brain Sciences, Leipzig, Germany

Corresponding Author: Timo T. Schmidt (timo.t.schmidt@fu-berlin.de)

ABSTRACT

The thalamus is primarily known as a relay for sensory information; however, it also critically contributes to higher-order cortical processing and coordination. Thalamocortical hyperconnectivity is associated with hallucinatory phenomena that occur in various psychopathologies (e.g., psychosis, migraine aura) and altered states of consciousness (ASC; e.g., induced by psychedelic drugs). However, the exact functional contribution of thalamocortical hyperconnectivity in forming hallucinatory experiences is unclear. Flicker light stimulation (FLS) can be used as an experimental tool to induce transient visual hallucinatory phenomena in healthy participants. Here, we use FLS in combination with fMRI to test how FLS modulates thalamocortical connectivity between specific thalamic nuclei and visual areas. We show that FLS induces thalamocortical hyperconnectivity between lateral geniculate nucleus (LGN), early visual areas, and proximal upstream areas of the ventral visual stream (e.g., hV4, VO1). Further, an exploratory analysis indicates specific higher-order thalamic nuclei, such as anterior and mediodorsal nuclei, to be strongly affected by FLS. Here, the connectivity changes to upstream cortical visual areas directly reflect a frequency-dependent increase in experienced visual phenomena. Together, these findings contribute to the identification of specific thalamocortical interactions in the emergence of visual hallucinations.

Keywords: visual hallucinations, flicker light stimulation, altered states of consciousness, thalamocortical connectivity, thalamic nuclei, functional connectivity, visual hierarchy

1. INTRODUCTION

The functional role of the thalamus goes beyond a relay for sensory information to the cortex. Indeed, no more than 20% of thalamic volume are primary sensory nuclei (Hádinger et al., 2023; Rovó et al., 2012). With complex connectivity throughout the neocortex, the thalamus contributes to higher-order processing, cognition and is also thought to coordinate information availability across cortices (Halassa & Sherman, 2019; Sherman & Guillery, 2006). Correspondingly, thalamocortical hyperconnectivity has been related to various pathologies, such as psychosis (Avram et al., 2021; Ramsay, 2019), epilepsy (Chen et al., 2021; Kim et al., 2014), and migraine (Bolay, 2020; Martinelli et al., 2021; Tu et al., 2019), and during diverse

Received: 26 July 2023 Revision: 26 October 2023 Accepted: 30 October 2023 Available Online: 3 November 2023

altered states of consciousness (ASC; e.g., induced by psychoactive drugs (Carhart-Harris et al., 2016; Müller et al., 2017; Preller et al., 2019)), all of which involve hallucinatory experiences (consider also Hirschfeld & Schmidt, 2021; Hirschfeld et al., 2023; Prugger et al., 2022; Schmidt & Majić, 2017). However, the exact functional contributions of thalamocortical hyperconnectivity to the emergence of hallucinatory phenomena are unclear. Previous reports are limited in the specificity of distinct thalamic nuclei contributions. Here, we utilize flicker light stimulation (FLS) in combination with fMRI to induce transient visual hallucinations in healthy participants and test for the differential modulation of functional connectivity between thalamic nuclei and visual areas.

The neural mechanisms of visual hallucinations are difficult to investigate empirically as their involvement in pathologies is spontaneous and they co-exist with other neurophysiologic symptoms (Rogers et al., 2021). Furthermore, the use of medication in patient populations may have confounding effects on observed connectivity patterns that are difficult to identify and control (Lieslehto et al., 2021). This makes it important to identify an experimental tool that can selectively induce visual hallucinatory phenomena in healthy participants. FLS applies stroboscopic light, primarily at alpha frequency (8-12 Hz), over closed eyes to elicit visual hallucinatory perception within seconds of stimulus onset. FLS-induced hallucinations include the perception of simple geometric patterns, motion, and colors (Allefeld et al., 2011; Amaya et al., 2023; Bartossek et al., 2021; Montgomery et al., 2023), which hold close similarity to the content of visual hallucinations reported in migraine (Cowan, 2013; Panayiotopoulos, 1994; Richards, 1971; Schott, 2007; Wilkinson, 2004), epilepsy (Panayiotopoulos, 1994), psychedelic experiences (Bartossek et al., 2021; Klüver, 1966; Lawrence et al., 2022), and Charles Bonnet Syndrome (Ffytche, 2005; Jan & Castillo, 2012). FLS rhythmicity, frequency, and brightness can be closely controlled in an experimental setting (Rogers et al., 2021), making it an optimal tool to investigate neural mechanisms of visual hallucinations.

By identifying which thalamic nuclei display altered connectivity with the cortex during visual hallucinations, the functional role of thalamocortical dysconnectivity can be indicated. The lateral geniculate nucleus (LGN) is the first-order thalamic nucleus for visual input and has bidirectional connections with V1. Here, feedforward thalamocortical projections relay visual information from the retina. Feedback corticogeniculate connections modulate activity of the LGN via inhibitory interneurons (Sherman & Guillery, 2006). These pathways determine LGN activity by streaming visual information (e.g., stimulus features (Andolina et al., 2007)) and integrating extravisual modulations (e.g., attentional (Reinhold et al., 2023)) (see Briggs, 2020, for review). The cortico-striato-thalamo-cortical (CSTC) model proposes that drug- and pathology-induced hallucinations arise from thalamocortical hyperconnectivity (Geyer & Vollenweider, 2008; Preller et al., 2019; Vollenweider & Geyer, 2001). With the perspective of the thalamus as a sensory gate, its contribution to hallucinations is mostly attributed to dysfunctional gating, leading to "sensory flooding" (Geyer & Vollenweider, 2008) and consequent cortical misinterpretation of sensory signals. In line with this suggestion, the thalamus was found to have increased connectivity with the occipital cortex in patients with schizophrenia (Anticevic, Yang, et al., 2014) and during psychedelic experiences (Müller et al., 2017), which may reflect reduced thalamic gating capacities of the LGN to visual information passing to the cortex.

Recently, there has been more attention on the differential roles of first-order and higher-order thalamic nuclei in the generation of visual hallucinations (Vollenweider & Preller, 2020), which is facilitated by methodological advances allowing for parcellation of thalamic nuclei (Iglehart et al., 2020; Johansen-Berg et al., 2005). Higher-order nuclei do not receive input from sensory organs, instead, they orchestrate cortico-cortical communication and modulate activity of other thalamic nuclei (Sherman, 2016; Sherman & Guillery, 2006). With regards to visual processing, the inferior and lateral pulvinar are a group of higher-order nuclei with pronounced bidirectional anatomic connections to V1, V2, and V4 (Gattass et al., 2014; Shipp, 2003; Soares et al., 2001), contributing to visual processing and attention (Adams et al., 2000; Benevento & Rezak, 1976; Gattass et al., 2017; Guedj & Vuilleumier, 2020; Kaas & Lyon, 2007; Saalmann et al., 2012). They are associated with the generation of hallucinatory phenomena as they show a reduction in volume, neuronal number, and neuronal size in individuals with schizophrenia (Byne et al., 2002; Danos et al., 2003) and dementia with Lewy Bodies (symptoms includes visual hallucination) (Erskine et al., 2017). However, medication and comorbidities may introduce confounds to the observed neurophysiological states, making it uncertain whether pulvinar nuclei have specific functional contributions to hallucinatory experiences. Still, the inferior and lateral pulvinar are candidate higher-order thalamic nuclei that may contribute to the emergence of FLS-induced visual hallucinatory phenomena.

When aiming to identify the functional role of thalamocortical interactions in the emergence of visual hallucinations, it is relevant to test for differential contributions of visual stream areas with regards to their hierarchical organization. The visual cortex comprises early visual cortices (EVC: V1-V3), which are typically defined by their retinotopic representation of the visual field (Engel et al., 1997; Sereno et al., 1995), and upstream visual areas, which show less pronounced retinotopy and are commonly described by their selective response to specific features of visual input, such as the activation preference for motion (hMT/V5; Zeki et al., 1991), shape (hV4/LO2; Grill-Spector et al., 1998; Malach et al., 1995; Silson et al., 2013), color (hV4/VO1; Persichetti et al., 2015), and orientation (LO1; Silson et al., 2013). One previous EEG study indicated an increase in V4 activity during FLS (Ffytche, 2008), which may relate to the increased subjective intensity of seeing shapes and colors. However, it is likely that altered processing in multiple visual areas relates to FLS-induced effects and the exact functional contributions of cortical areas along the visual hierarchy have not yet been reported.

In this study, we test whether FLS-induced visual hallucinations relate to altered thalamocortical connectivity, and which thalamic nuclei and visual areas are primarily modulated. We use constant light, 3 Hz FLS and 10 Hz FLS, expecting that 10 Hz FLS will induce stronger visual hallucinatory phenomena than 3 Hz FLS and constant light, as previously reported (see Amaya et al., 2023; Bartossek et al., 2021). We acquired resting state fMRI data and use the Automated Anatomical Labelling Atlas 3 (AAL3; Rolls et al., 2020) for thalamus parcellation and a volume-based maximum probability map of visual topography (Wang et al., 2015) for parcellation of visual areas. We hypothesize that LGN will show hyperconnectivity with EVC for 3 Hz and 10 Hz FLS, as they receive excitatory signals from the retina and therefore synchronize to the periodic visual stimulus. For higher-order visual regions, as well as higher-order thalamic nuclei (e.g., inferior and lateral pulvinar), we expect to find a parametric modulation of connectivity by the experimental conditions, such that constant light will induce hypoconnectivity, as found in previous work (Schmidt et al., 2020), and FLS will induce frequency-dependent increases in connectivity, whereby 10 Hz produces the strongest coupling. We expect to see these parametric effects in both dorsal and ventral streams of the visual system, as FLS is known to induce hallucinatory perception of motion (Amaya et al., 2023), and geometric shapes and colors (Amaya et al., 2023; Bartossek et al., 2021), pertaining to the dorsal and ventral stream respectively. Thereby, changes in connectivity should resemble the intensity of subjective hallucination experience.

2. METHODS

2.1. Participants

Twenty-four German speakers with no history of psychiatric or neurological disorders participated in the experiment (14 female; age range 20-41 years, mean ± standard deviation = 28 ± 5.7 years). All participants were right-handed according to the Edinburgh Handedness Inventory (Oldfield, 1971) (mean laterality quotient (M ± SD) = 75.6 ± 21.5), although right-handedness was not a requirement for participation. Social media and student mailing lists within the Freie Universität, Berlin were used for recruitment. Participants were informed about the study aims and background, such as possible risks of FLS, before giving written consent. The study was approved by the ethics committee of the Charité Universitätsmedizin Berlin (application number: EA4/143/18). All procedures were consistent with the guidelines included in the "Declaration of Helsinki—Ethical Principles for Medical Research Involving Human Subjects."

2.2. Flicker light stimulation

For presentation of the light stimulation, we used the light device Lucia N°03 (Light Attendance GmbH, Innsbruck, Austria), which has been developed to evoke hypnagogic visual impressions by intermittent light stimulation. It is equipped with one halogen lamp that is used for constant light stimulation and eight LEDs to apply FLS with high precision timing and luminance via a programmable interface. Three light stimulation conditions were used: (1) Constant light stimulation at full intensity through a halogen lamp; (2) 3 Hz; and (3) 10 Hz FLS as 50% ON/50% OFF times with LED light at maximum intensity, as previously applied (Bartossek et al., 2021; Schwartzman et al., 2019). To apply light stimulation inside the fMRI scanner, the light device was mounted on an aluminum stand close to the end of the gantry at 150 ± 2 cm from the participants' eyes. To make the light stimulation comparable to a previous phenomenological study where the lamp was positioned 50 cm from participants' eyes (Bartossek et al., 2021), two lenses were introduced into the MRI-mirror system to collect and focus the light (Fig. 1A) to deliver approximately the same amount of light to the eyes. To protect the light device from overheating (as the in-built ventilation did not work in the

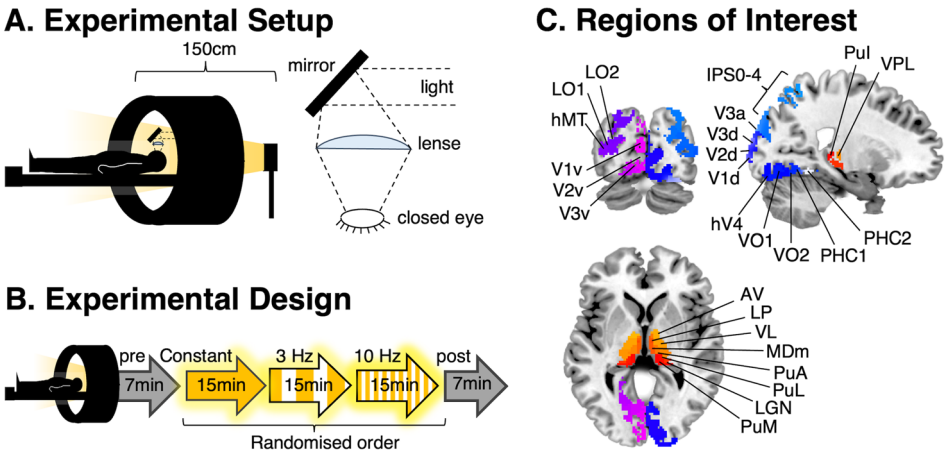

Fig. 1. (A) Illustration of the setup inside the MRI scanner. FLS with the Lucia N°03 light device is optimized for stimulation with 50 cm distance from the eyes. Inside the scanner, the lamp was positioned at the end of the gantry at approximately 150 cm from the eyes and lenses were used to focus light back onto the eyes to obtain the same amount of light as outside of the scanner. (B) The fMRI session comprised five closed-eye resting-state scans. The experimental conditions, constant light, 3 Hz and 10 Hz (15 minutes each) were presented in a randomized order, while the pre- and post-scans (7 minutes each) consisted of closed-eye rest for baseline measurements. (C) Regions of interest (ROIs) were extracted from AAL3 for thalamus parcellation (Rolls et al., 2020) and a volume-based maximum probability map of visual topography (Wang et al., 2015) for cortical parcellation. Thalamic ROIs, as labeled, are anteroventral (AV), lateroposterior (LP), ventrolateral (VL), mediodorsal medial (MDm), anterior pulvinar (PuA), lateral pulvinar (PuL), lateral geniculate nucleus (LGN), medial pulvinar (PuM), inferior pulvinar (Pul), and ventroposterolateral (VPL) nuclei. Additional thalamic ROIs not displayed are mediodorsal lateral (MDl), intralaminar (IL), ventroanterior (VA), and medial geniculate nuclei (MGN). Cortical ROIs of visual topography are split into the dorsal stream (V1d, V2d, V3d, V3a, V3b, LO1, LO2, hMT), ventral stream (V1v, V2v, V3v, hV4, VO1, VO2, PHC1, PHC2), and parietal stream (IPS0-4, SPL1, FEF). Cortical ROIs not displayed are V3b, SPL1, and FEF.

magnetic field), a custom-made air cooling was used that comprised an industrial vacuum cleaner positioned outside of the shielded MRI room to deliver cold air via an extension hose to the light device.

2.3. Study design and procedure

To minimize risk of aversive effects of FLS, all participants underwent a preliminary semi-structured video-interview with a psychologist to identify any acute mental disorders, consumption of psychotropic medication, and/or pregnancy. Thereafter, participants were screened for indications of photosensitive epilepsy based on electroencephalography (EEG) and were shortly presented FLS of each experimental condition to be familiarized with the procedures and setup. All measurements were conducted at the Center for Cognitive Neuroscience Berlin (CCNB), Freie Universität Berlin.

The scanning session comprised five scans: pre- and post-scans, each lasting seven minutes and consisting of closed-eye rest in darkness, and three light stimulation scans lasting 15 minutes each (Fig. 1B). After every scan, the participants were asked six questions about their subjective experiences (see below) and verbally responded via the speaker system of the scanner. An anatomical scan was performed before participants were released from the scanner and experiment.

2.4. FLS-induced phenomenology

Phenomenological aspects of the FLS-induced state were retrospectively assessed using six questions of the Altered States of Consciousness Rating Scale (ASC-R; Dittrich, 1998), which were previously identified as most characteristic of the subjective experience (Bartossek et al., 2021). The questions were applied in German, taken from the original version of the 5D-ASC (Dittrich, 1998) and participants were asked to rate by verbally naming a value from 0-100% for how much the following statements apply: (1) *Ich fühlte mich schläfrig* English: *I felt sleepy,* (2) *Ich fühlte mich körperlos* English: *I had the impression I was out of my body,* (3) *Wie im Traum waren Raum und Zeitgefühl verändert* English: *My sense of time and space was altered as if I was dreaming*, (4) *Ich fühlte*

mich wie in einer wunderbaren anderen Welt English: *I felt I was in a wonderful other world*, (5) *Ich sah regelmäßige Muster*, English: *I saw regular patterns* (Note: In the original version the statement continues as: *… with closed eyes or in complete darkness*), and (6) *Ich sah Farben vor mir* English: *I saw colours* (Note: In the original version the statement continues as: *… with closed eyes or in complete darkness*). We ran one-way repeated-measures ANOVAs to test the effect of experimental condition on ASC-R questionnaire ratings using the *rstatix* package in Rstudio (v2022.07.2). As distribution of ratings had a tendency for skewedness (e.g., positive skew for pre- and post-scans), significant ANOVA results were additionally confirmed using non-parametric Kruskal-Wallis testing. Post-hoc t-tests were Bonferroni-corrected to .005 to account for 10 comparisons across five groups.

2.5. fMRI scanning

Participants were scanned using a 3 T Siemens TIM Trio MRI scanner equipped with a 32-channel head coil (Siemens Medical, Erlangen, Germany). For resting-state fMRI images, a T2*-weighted echo planar imaging (EPI) sequence was used (37 axial slices acquired interleaved, in-plane resolution is 3 mm^2, slice thickness = 3 mm, flip angle (FA) = 70°, 20% gap between slices, repetition time (TR) = 2000 ms, echo time (TE) = 30 ms). A structural image was acquired for each participant using a T1-weighted image acquired with Magnetisation prepared rapid gradient-echo (MPRAGE) sequence (TR = 1900 ms, inversion time = 900 ms, TE = 2.52 ms, FA = 9°, voxel size = 1 mm^3). Head motion was minimized using cushioned supports to restrict movement.

2.6. MRI data pre-processing

Data were pre-processed and analyzed using a custom-built resting-state data analysis pipeline within SPM12 (www.fil.ion.ucl.ac.uk/spm/). The anatomical T1-images were normalized to MNI152 space using the segmentation approach, by estimating a nonlinear transformation field, which is then applied to the functional images. Slice time correction and realignment was applied to the functional data before spatial normalization to MNI152 space using unified segmentation in SPM12, which includes reslicing to an isometric 2 mm voxel size (Ashburner &Friston, 2005). The frame-wise displacement (FD) was calculated for each scan using BRAMILA tools (Power et al., 2012) and volumes that exceeded a threshold of 0.4 mm were masked during following analysis steps (*"scrubbing"*). For all runs and participants, the mean percentage of scrubbed volumes was 2.6 ± 4.4% (M ± SD). All runs had less than 20% scrubbed volumes, with the exception of two runs from one participant where 26.9% and 22.2% of volumes were scrubbed. A control group-level analysis revealed that the exclusion of this dataset did not affect the main reported results, and therefore the data of this participant were kept. Principal component analysis (CompCor) was done using the Data Processing and Analysis of Brain Imaging (DPABI) toolbox (http://rfmri.org/dpabi; Behzadi et al., 2007) within the CSF/white matter mask on the resting-state data to estimate nuisance signals. Anatomical masks for CSF, white, and gray matter were derived from tissue-probability maps provided in SPM12. Smoothing was performed with a 3 mm FWHM Gaussian kernel, to retain high spatial specificity of small ROIs within the thalamus. The first five principal components of the CompCor analysis, six head motion parameters, linear and quadratic trends, as well as the global signal were used as nuisance signals to regress out associated variance. The removal of global signal changes has been controversially discussed in resting-state fMRI literature with arguments for and against (see K. Murphy & Fox, 2017, for overview). It has been particularly discussed for pharmacological studies (e.g., Carhart-Harris et al., 2012; Vollenweider & Preller, 2020), in which changes in blood flow, blood pressure, breathing rate, and other physiologic parameters might account for some aspects of ROI-to-ROI correlations. Until conclusive interpretations of such differences are revealed, it is suggested to report data with and without global signal regression (Vollenweider & Preller, 2020). Therefore, we additionally report baseline measurements and connectivity analyses without GSR in the Supplement (S1-4). Finally, the toolbox REST (www.restfmri.net) was used for temporal band-pass filtering (0.01-0.08 Hz).

2.7. ROI-to-ROI correlation analysis

We used the AAL3 (Rolls et al., 2020) to define anatomical ROIs for thalamus parcellation (14 thalamic nuclei for each hemisphere) and a volume-based maximum probability map of visual topography for cortical parcellation (23 visual areas for each hemisphere; see Fig. 1C) (Wang et al., 2015). Using probability maps of V1 and V2, overlapping ROIs at the midline were resolved by assigning voxels to the region with the highest probability. Of thalamic ROIs, the Reuniens nucleus is only 8 mm^3 and was not included in our analyses. Additionally, when the cortical maximum probability map was

resliced to 2 mm^3, hMST and IPS5 were no longer present in one hemisphere. For consistency, these ROIs were removed bilaterally.

For each ROI, mean BOLD time courses were extracted and temporal ROI-to-ROI Pearson correlations were calculated and subsequently Fisher z-transformed. For all ROI-to-ROI pairs, we averaged the correlation coefficients of pre- and post-scans and then computed the difference with experimental conditions via subtraction of matrices. We took the mean of correlation coefficients for ipsilateral connections (e.g., left LGN and left V1v averaged with right LGN and right V1v), as anatomical thalamocortical connections are predominantly ipsilateral, to give one bilateral functional correlation coefficient for each pair of ROIs. Non-averaged unmasked ipsilateral and contralateral connectivity matrices are presented in the Supplement (S5-7), demonstrating major consistency across all four connection types. To test for specific changes within thalamus and visual areas, we ran repeated-measures ANOVAs with condition as a fixed effect and connectivity changes as the dependent variable. We selected 16 visual areas to test: 8 within the ventral stream (V1v, V2v, V3v, hV4, VO1, VO2, PHC1, PHC2) and 8 within the dorsal stream (V1d, V2d, V3d, V3a, V3b, LO1, LO2, hMT), as classified by Wang et al. (2015). We conducted the analyses for LGN, inferior, and lateral pulvinar. We Bonferroni-corrected the alpha threshold to .003 (.05/16) to correct for 16 repeated-measures ANOVAs for every thalamic nucleus. When tests were significant, post-hoc t-tests were used to determine the differences between condition groups. The alpha threshold of post-hoc t-tests was Bonferroni-corrected to .017 (.05/3) to account for three comparisons across experimental conditions. Thereafter, we further explored the ROI-to-ROI connectivity matrices of all thalamic and visual ROIs to identify if functional connectivity with any other thalamic nuclei or visual areas appeared to be modulated by FLS.

2.8. Testing the relationship between subjective experience and connectivity changes

To test for the relationship between subjective experience and connectivity changes, we selected ratings of "I saw regular patterns" and "I saw colours" to reflect the intensity of visual phenomena. Using paired t-tests, we tested whether the distribution of ratings between the two items were different for each condition. As these tests were nonsignificant, we took the average of seeing patterns and seeing colors for each participant as the measure for visual hallucination intensity. We subtracted the average of pre- and post-ratings from those of each experimental condition. From here, we ran linear mixed-effects models with change in subjective ratings as a fixed effect and change in functional connectivity as the dependent variable. Participants were included as a random effect. Models with random intercept only had better fit (i.e., lower Akaike Information Criterion values) than random intercept and random slope models, and therefore models were run with random intercepts only. Following our hypotheses, we ran this test for connectivity changes between LGN, inferior pulvinar, lateral pulvinar, and 16 visual subregions, thus Bonferroni-correcting the alpha threshold to .003 (.05/16). To assess whether the relationship was specific to visual effects, we additionally ran the linear mixed models with other ASC ratings as fixed effects (e.g., "I had the impression I was out of my body"). All analyses were conducted using the *lme4* package in Rstudio (v2022.07.2). To test the underlying assumptions of linear mixed modeling, Normal Q-Q plots were used to assess whether residuals of the linear mixed model fit followed a Gaussian distribution. Homoscedasticity was confirmed by plotting the residuals against predicted values and observing no pattern in the noise distribution. The assumption of independence was addressed by including participants as a random effect in the linear mixed model.

3. RESULTS

3.1. FLS-induced subjective experience

We assessed the subjective experience following each scanning session (including pre/post scans) to test whether reported effects induced by the experimental conditions were comparable to previous findings where FLS was applied outside the MRI scanner (Amaya et al., 2023; Bartossek et al., 2021). Using ASC-R scores from each session, we ran 5 x 1 repeated-measures ANOVAs to test the effect of condition on ASC ratings (Fig. 2). We found a significant effect of experimental condition on ratings of "I felt I was in a wonderful other world" ($F(4, 92) = 9.83$, $p < .001$), "My sense of time and space was altered as if I was dreaming" ($F(4, 92) = 7.12$, $p < .001$), and "I had the impression I was out of my body" ($F(4, 92) = 5.37$, $p < .001$), where post-hoc paired t-tests revealed that 10 Hz elicited higher ratings than pre- and post-resting scans ($p < .05$). Further, there was a significant effect of experimental condition on ratings of "I saw patterns" ($F(2.09, 48.03) = 104.53$, $p < .001$) and "I saw

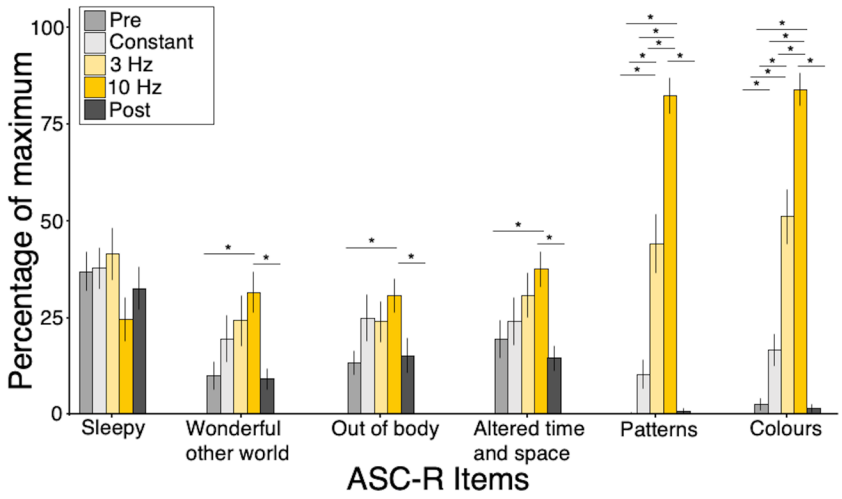

Fig. 2. Mean scores of ASC-R items for each experimental condition, indicating no differences on wakefulness across conditions, minor parametric effects on general ASC phenomena, and a strong modulation of visual phenomena. Effects tested via one-way repeated-measures ANOVAs; post-hoc paired t-test significance is corrected to $p < .005$ (.05/10 for 10 comparisons) and results that survived Bonferroni correction are marked with a star (*). Standard error is depicted by error bars.

colours" ($F(2.2, 50.71) = 88.78$, $p < .001$), where post-hoc paired t-tests showed that all experimental conditions were significantly different from each other and 10 Hz generated the highest ratings ($p < .001$) (Fig. 2). Non-parametric Kruskal-Wallis testing confirmed all ANOVA results (Out of body: $H(4) = 14.23$, $p = .006$; Altered time and space: $H(4) = 15.88$, $p = .003$; Wonderful other world: $H(4) = 16.79$, $p = .002$; Patterns: $H(4) = 87.61$, $p < .001$; Colours: $H(4) = 87.84$, $p < .001$), together showing that FLS inside the MRI scanner robustly induced hallucinatory experiences in all participants, with 10 Hz stimulation eliciting the highest intensity of subjective experience.

3.2. Changes in functional connectivity between LGN and visual areas

We tested for effects of FLS (3 Hz, 10 Hz) and constant light on connectivity changes from baseline between LGN nuclei and 16 visual areas using repeated-measures 3 x 1 ANOVAs (note that for every participant we averaged connectivity changes across ipsilateral connections; see methods). Alpha is Bonferroni-corrected to .003 (.05/16). We found an increase in connectivity strength for 3 Hz and 10 Hz compared to baseline (average of pre- and post-scans), however 3 Hz and 10 Hz were not different from each other (Fig. 3). Specifically, there was a significant effect of experimental condition on connectivity changes between LGN and V1v ($F(2, 46) = 15.89$, $p < .001$), V1d, $F(2, 46) = 19.23$, $p < .001$), V2v ($F(2, 46) = 24.58$, $p < .001$), V2d ($F(2,46) = 26.17$, $p < .001$), V3v ($F(2,46) = 20.17$, $p < .001$), V3d ($F(2,46) = 16.09$, $p < .001$), which encompasses all early visual areas. In addition, there was a significant effect of experimental condition on connectivity changes with hV4 ($F(2, 46) = 12.16$, $p < .001$), VO1 ($F(2, 46) = 6.95$, $p = .002$) and V3a ($F(2, 46) = 7.79$, $p = .001$), whereby 10 Hz FLS induces the strongest coupling, followed by 3 Hz while constant light induced a weak decoupling.

3.3. Changes in functional connectivity between pulvinar and visual areas

Using the same treatment of data as for the LGN, we tested for effects of experimental condition on connectivity changes between inferior and lateral divisions of the pulvinar and 16 subregions of the visual cortex. Using repeated-measures 3 x 1 ANOVAs, we found no significant effects of condition on connectivity changes with inferior pulvinar across all tested visual areas, which is evident in Figure 3. For the lateral pulvinar, a significant effect of condition was revealed for connectivity changes with V1d ($F(2,46) = 7.12$, $p = .002$) and V2v ($F(2,46) = 7.50$, $p = .002$), whereby post-hoc t-tests showed that 10 Hz and 3 Hz induced stronger coupling than constant light ($p < .05$) (Fig. 3).

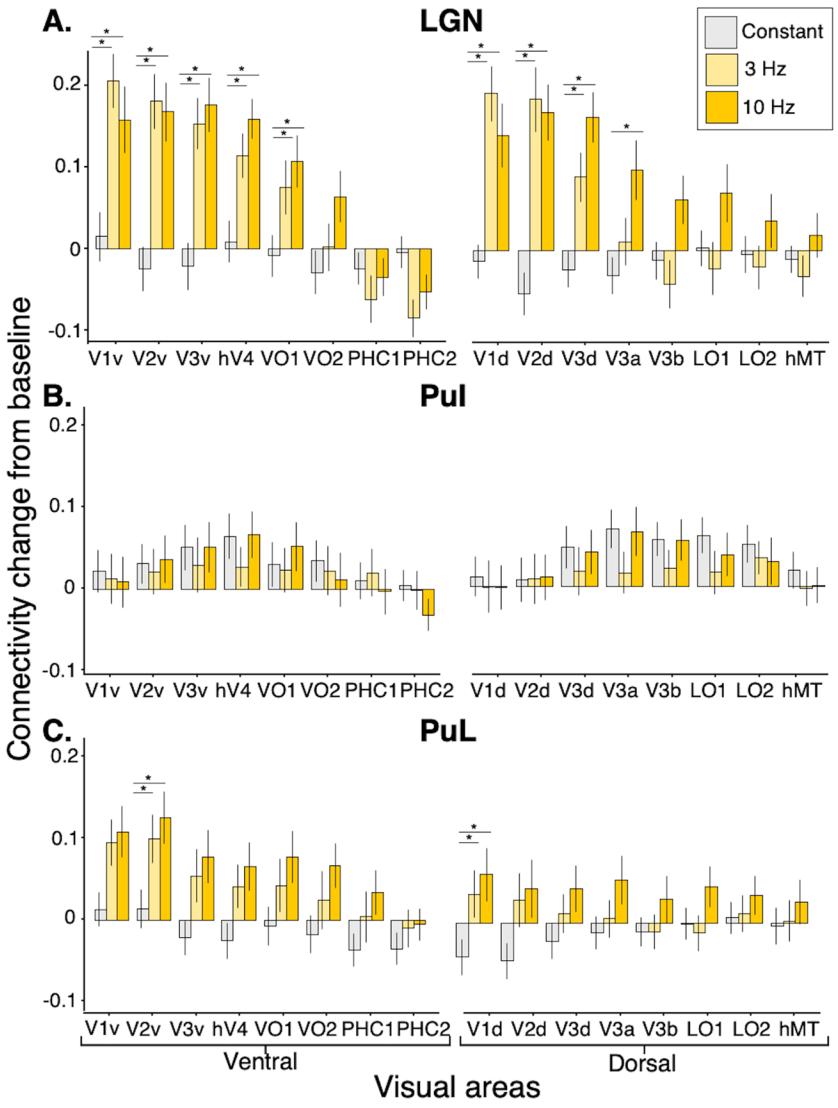

Fig. 3. Effects of FLS on functional connectivity changes compared to baseline (average of pre- and post-scans) between visual areas and (A) LGN, (B) inferior pulvinar (PuI), and (C) lateral pulvinar (PuL). Visual areas are grouped into ventral and dorsal visual streams, as presented by Wang et al. (2015). Of the repeated-measures ANOVAs that returned significant effects of condition on connectivity change from baseline ($p < .003$), post-hoc paired t-tests indicate differences between conditions, where alpha is Bonferroni-corrected to .017 (.05/3) and tests that survive correction are marked with a star (*). There is a strong modulation of condition on connectivity increases between LGN and EVC, and proximal upstream visual areas of dorsal (V3a) and ventral (hV4, VO1) streams. 3 Hz and 10 Hz induce LGN hyperconnectivity to the same degree for EVC, however for higher areas of the dorsal stream (V3a, V3b, LO1), LGN hyperconnectivity is only apparent during 10 Hz FLS. There is no significant effect of light stimulation on connectivity changes between inferior pulvinar and visual areas, while lateral pulvinar shows a similar pattern of connectivity changes as LGN with visual areas, albeit less strong.

3.4. Association of connectivity strength with subjective experience

We ran linear mixed models with rating as a fixed effect and participant-specific random intercepts to determine if ASC-R mean ratings of experienced visual effects (i.e., mean of "I saw patterns" and "I saw colours"; see Methods) could predict changes in functional connectivity between ROIs. Alpha was Bonferroni-corrected to .003 to account for the comparison of 16 models for each group (i.e., 16 visual areas for LGN, lateral pulvinar, and inferior pulvinar). We found that subjective ratings significantly predicted increases in connectivity between the LGN and V2v ($p < .001$; $R^2m = 0.14$; $R^2c = 0.45$), V2d ($p < .001$;

R^2m = 0.15; R^2c = 0.44), V3v (p < .001; R^2m = 0.19, R^2c = 0.54), V3d (p < .001; R^2m = 0.26, R^2c = 0.59), hV4 (p < .001; R^2m = 0.21, R^2c = 0.49), VO1 (p = .002; R^2m = 0.12, R^2c = 0.55), VO2 (p = .001; R^2m = 0.10, R^2c = 0.48), V3a (p < .001; R^2m = 0.16, R^2c = 0.58) and V3b (p = .001; R^2m = 0.10, R^2c = 0.48). Furthermore, subjective ratings significantly predicted connectivity increases between lateral pulvinar and V1d (p < .001; R^2m = 0.10; R^2c = 0.56). We ran the same linear mixed models with ratings of "Wonderful other world," "Altered time and space," and "Out of body" as fixed effect variables and found they did not predict changes in connectivity between thalamic and visual regions. This further confirms the specificity of visual hallucinatory effects to connectivity changes between thalamus and visual cortices. Together, this shows that the subjective ratings associate more so with LGN interactions with upstream visual areas beyond V1, while connectivity between V1 and lateral pulvinar is significantly associated with subjective ratings.

3.5. Exploratory analysis of thalamocortical connectivity

To explore the whole connectivity profiles of thalamic nuclei, we plotted connectivity matrices with 14 thalamic ROIs from the AAL3 atlas (Rolls et al., 2020) and 23 cortical ROIs from the Wang et al. maximum probability map of visual topography (Wang et al., 2015). Figure 4 displays the ROI-to-ROI correlation coefficients of the experimental conditions subtracted by the averaged pre and post scans, thus showing the connectivity change induced by the conditions. We see strong hyperconnectivity between anterior (AV), ventral, and mediodorsal (MD) thalamic nuclei and cortical visual regions. Connectivity with upstream cortical visual regions, such as hV4, VO1, and V3a, shows more frequency-dependent effects (i.e., 10 Hz induces more coupling than 3 Hz) than EVC. We note that, as ventral nuclei (i.e., VA and VL) show similar changes in connectivity patterns and have anatomical proximity, we consider their effects collectively as a ventral group. Likewise, MDm and MDl are divisions of MD nuclei showing similar connectivity patterns and are therefore considered together as the MD region.

3.6. Exploratory analysis of visual area and thalamic interconnectivity

To explore interconnectivity profiles of visual and thalamic areas, we plotted masked interconnectivity matrices of 23 cortical and 14 thalamic ROIs, where only connectivity changes that were significantly different from baseline (p < .01) are displayed (Fig. 5). Figure 5A shows that 3 Hz and 10 Hz FLS leads to hyperconnectivity within EVC

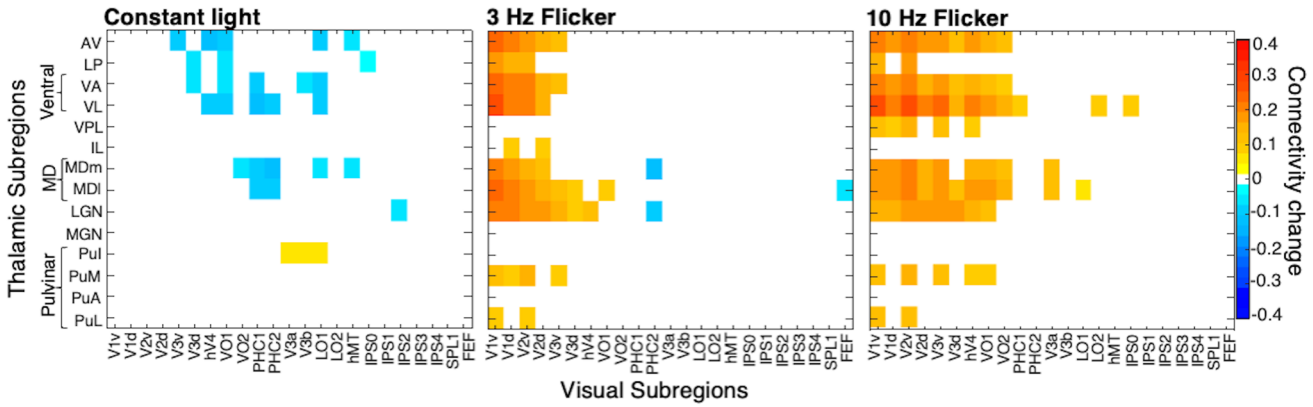

Fig. 4. Connectivity matrices for all visual areas and thalamic nuclei during constant light, 3 Hz and 10 Hz FLS, subtracted by the average of pre- and post-scans (closed-eye rest) to represent the connectivity change induced by the experimental conditions. A mask has been applied where only significant connectivity changes compared to baseline are shown, as determined by paired t-tests (alpha threshold of .01 to highlight most significant differences and to reduce noise). VA and VL (ventral group) display similar connectivity patterns, while VL shows marginally stronger connectivity at 10 Hz. Likewise, medial and lateral divisions of MD nuclei show similar connectivity patterns and can be collectively considered as the MD region. With this clustering, we observe that AV, ventral, and MD thalamic regions display the greatest frequency-dependent effects of FLS on connectivity changes with visual areas, in that 10 Hz induces the strongest coupling that is additionally evident in upstream visual areas of both ventral (e.g., VO2) and dorsal (e.g., V3a) visual streams. Meanwhile, we see overall hypoconnectivity in the constant light condition.

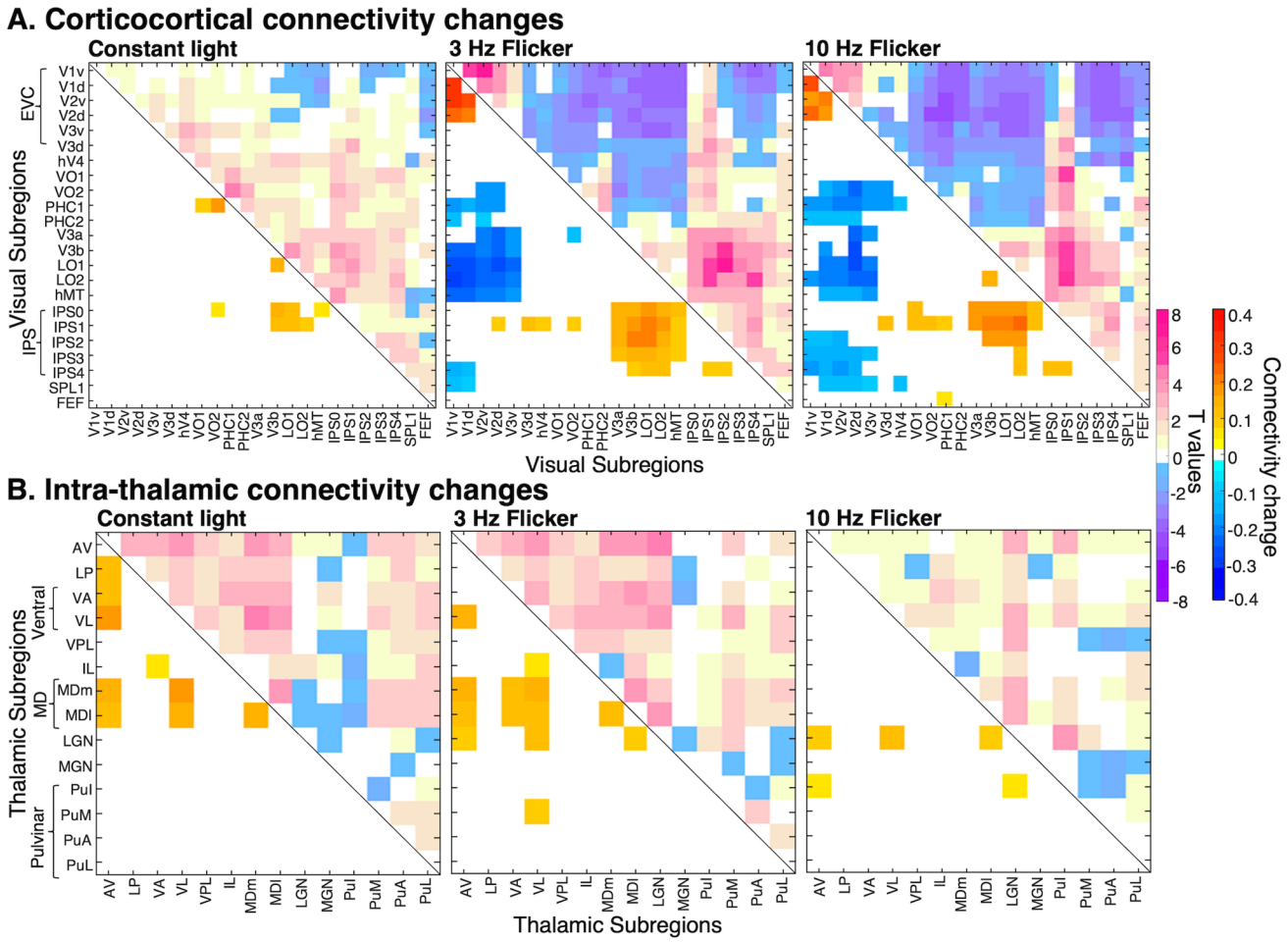

Fig. 5. (A) Connectivity changes between visual areas during constant light, 3 Hz and 10 Hz FLS, as compared to pre- and post-scans. Upper half of matrices shows t values of paired t-tests; lower half shows connectivity changes (masked at $p < .01$, where paired t-tests revealed a significant difference between connectivity in experimental condition versus baseline). There are two groups of hyperconnectivity: within EVC and between upstream visual areas (e.g., LO1, hMT) and IPS, while these groups are decoupled from each other. (B) Connectivity changes within the thalamus. The connectivity changes in the 10 Hz condition are confined to relevant areas (i.e., LGN, AV, ventral, and MD nuclei), which supports that the applied parcellation yields region-specific effects. If ROIs were to reflect the same underlying signals, one would expect an overall increase in connectivity between thalamic subfields. Thalamocortico-thalamic connections likely drive increased LGN connectivity with other thalamic nuclei (i.e., AV, ventral, and MD nuclei), such that the signal passes from LGN via visual cortices to higher-order thalamic nuclei.

(i.e., V1-V2) but hypoconnectivity between EVC and higher visual areas of ventral (e.g., VO2, PHC), dorsal (e.g., V3a, hMT), and parietal (i.e., IPS) streams. Meanwhile, higher visual areas show increased coupling to each other (e.g., LO2 and IPS). Interconnectivity matrices of thalamic ROIs display a few changes in connectivity amongst thalamic nuclei, especially at 10 Hz FLS (Fig. 5B).

4. DISCUSSION

We tested the effects of FLS on functional connectivity between anatomically specified thalamic nuclei and visual areas. We found that FLS induced hyperconnectivity between the LGN and early visual cortices (EVC: V1-V3), independent of flicker frequency. Meanwhile, upstream visual areas show a differential effect of flicker frequency on LGN connectivity, in that coupling was strongest for 10 Hz. Similarly, FLS induced a frequency-dependent increase in participant ratings of visual hallucinations ("I saw colours" and "I saw patterns"), which replicates previous findings (Amaya et al., 2023; Bartossek et al., 2021). The intensity of visual phenomena was associated with the strength of connectivity changes between LGN and higher visual areas, especially for V3 and hV4, suggesting

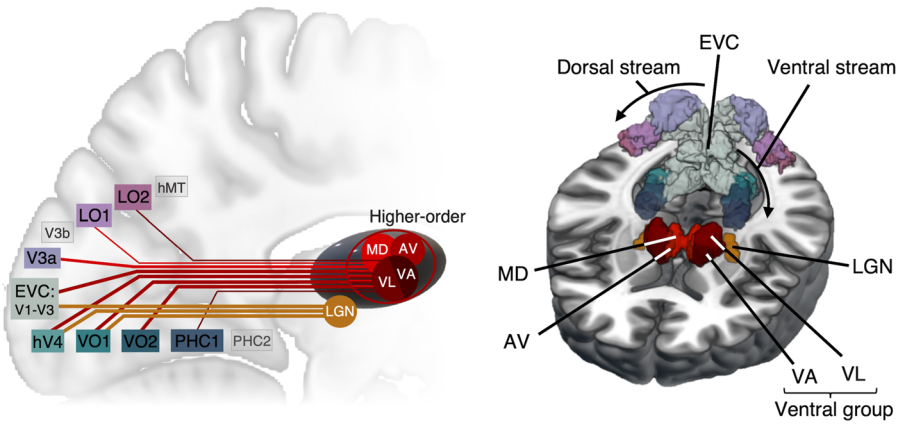

Fig. 6. Summary of thalamocortical functional connections changes during 10 Hz FLS. Red and orange lines represent functional hyperconnectivity compared to baseline for higher-order (non-sensory) and first-order (sensory; LGN) thalamic regions, respectively. The strength of correlation change is depicted by line thickness. During FLS, the LGN shows connectivity increases to early visual cortices (EVC; V1-V3) and proximal upstream areas of the ventral stream (i.e., hV4, VO1). We found that anterior (AV), ventral (VL and VA), and mediodorsal (MD) higher-order thalamic nuclei display increased coupling with visual areas along ventral and dorsal visual streams (Note: the higher-order contributions of ventral nuclei are to date unclear). As these nuclei do not receive direct driving retinal inputs, they are most likely driven by inputs from EVC. While the directionality of effects in higher-order regions is speculative, our findings may indicate that AV, ventral, and MD nuclei take an orchestrating role for information flow across cortical regions.

that effects are not only driven by a simple feedforward mechanism from LGN to V1, but rather arise from a modulation of upstream visual areas. FLS additionally induced weak thalamocortical hyperconnectivity with the lateral pulvinar but had no effect on the inferior pulvinar. Hyperconnectivity between lateral pulvinar and V1 was associated with subjective ratings, which may correspond to a top-down modulatory influence of the pulvinar on V1. When exploring connectivity changes across all thalamic nuclei of the AAL3 atlas, we found stronger frequency-dependent modulations of connectivity between AV, ventral, and MD thalamic nuclei and visual areas. The connectivity changes induced by 10 Hz FLS are summarised in Figure 6. Moreover, we explored corticocortical connectivity changes between visual areas and observed two groups of hyperconnectivity: (1) within EVC and (2) between upstream visual areas and intraparietal sulcus (IPS), while these groups were decoupled from each other. Overall, we identify that hyperconnectivity between upstream visual areas, LGN, and other thalamic regions, such as AV, ventral, and MD nuclei, may be most relevant for the emergence of visual hallucinations.

4.1. Thalamocortical connectivity with LGN

FLS significantly increased connectivity between LGN and EVC, hV4, VO1, and V3a. This expected finding supports that rhythmic retinal activation propagates along dorsal (i.e., V3a) and ventral (i.e., hV4, VO1) visual streams. It is likely that driving inputs from the retina cause synchronization with LGN and subsequent visual areas via excitatory feedforward signaling, which manifests as an increase in functional connectivity, in the sense of entrainment. EEG studies have shown that periodic visual flicker at alpha frequency increases power at that frequency (Adrian & Matthews, 1934; Mathewson et al., 2012; Notbohm et al., 2016; Notbohm & Herrmann, 2016; Schwartzman et al., 2019), which is consistent with a neural field model showing that visual cortices selectively respond to periodic visual stimulation at alpha frequency (Butler et al., 2012; Pearson et al., 2016; Rule et al., 2011). Together, this aligns with findings that subjectively experienced FLS-effects are strongest in the alpha-frequency range shown here and previously (Amaya et al., 2023; Bartossek et al., 2021).

As there are rich feedback connections between visual cortices and thalamic nuclei (Budd, 2004; P.C. Murphy et al., 1999), an increase in functional connectivity likely encapsulates both feedforward and feedback processes. Indeed, it was recently shown that visual flicker induced phase-locking in LGN and cortical layers 4 and 5 of V1 (Schneider et al., 2023), which are involved in feedforward and feedback processes, respectively. The corticogeniculate inputs may refine the feedforward signals,

possibly through enhancing response precision and synchronizing LGN action potentials (Andolina et al., 2007; Briggs, 2020; Sillito et al., 1994), leading to the development of specific geometric patterns and distinct colors. Effective connectivity was recently assessed using regression Dynamic Causal Modelling (rDCM; Frässle et al., 2017, 2021) in an LSD study (Bedford et al., 2023), finding that LSD induced more directed connectivity from visual regions to thalamus than vice versa. However, the employed parcellation atlas did not allow further differentiation of involved thalamic subregions, and FLS likely exhibits different effective connectivity due to feedforward visual inputs. Therefore, while our data may represent changes to both feedforward and feedback interactions during FLS, future research should assess the weighting of these contributions to the resulting thalamocortical hyperconnectivity.

4.2. Thalamocortical connectivity with pulvinar

Due to the involvement of the pulvinar as a higher-order thalamic nucleus in visual processing (Adams et al., 2000; Benevento & Rezak, 1976; Guedj & Vuilleumier, 2020; Kaas & Lyon, 2007), we expected to find effects of FLS on thalamocortical connectivity with the inferior and lateral pulvinar. The lateral pulvinar demonstrated increased coupling with EVC, which was more apparent for ventral visual areas compared to dorsal areas (see Fig. 3). This reflects the major contribution of the lateral pulvinar to the ventral visual stream (Kaas & Lyon, 2007), which is responsible for shape and color recognition (Ungerleider & Haxby, 1994), possibly relating to the hallucinatory perception of patterns and colors, although tests of this association did not survive conservative Bonferroni correction. Additionally, there were no effects of FLS on inferior pulvinar connectivity, together showing that the effects of FLS on pulvinar connectivity were smaller than expected, especially when compared to other thalamic nuclei (see below). It is possible that the observed effects on the pulvinar can be assigned to contributions to visual attention (Gattass et al., 2014; Saalmann et al., 2012) rather than the subjective experience of visual hallucinatory phenomena.

4.3. Further thalamic nuclei displaying altered thalamocortical connectivity

Exploratory analyses of ROI-to-ROI connectivity highlighted three further thalamic subregions whose connectivity to visual areas seems to be modulated by FLS: (1) anterior nuclei, where all divisions of anterior nuclei are included in the AV region of the AAL3 atlas; (2) the ventral nuclei group, which includes VA and VL nuclei; and (3) MD nuclei. These thalamic regions showed hyperconnectivity with EVC during 3 Hz and 10 Hz FLS and hyperconnectivity with further upstream visual areas (e.g., V3a, VO2) for 10 Hz FLS only.

Anterior nuclei are critically involved in spatial navigation and memory (Roy et al., 2022; Safari et al., 2020). For example, they receive head direction signals through vestibular sensory inputs (Peyrache et al., 2019; Sharp et al., 2001; Taube, 2007). Within the anterior division, AV nuclei are linked to the visual cortex via connections to the retrospinal cortex (Lomi et al., 2023), which is thought to contribute to spatial organization in imagination (Botzung et al., 2008; D'Argembeau et al., 2008; Hassabis et al., 2007; Szpunar et al., 2007). Furthermore, a postmortem study of patients with schizophrenia found fewer thalamocortical projections in the AV nucleus bilaterally (Danos et al., 1998), suggesting a potential role in pathologic altered perceptual processing.

Within the ventral group, the VL nucleus has been associated with auditory-tactile synesthesia (Ro et al., 2007), despite being primarily known as a first-order relay for cerebellar inputs to motor cortices (Percheron et al., 1996). The ventral thalamic group was found to be hyperconnected with sensorimotor networks within psychosis (Avram et al., 2018) and following LSD administration (Avram et al., 2022), together indicating a contribution to altered perceptual processing. VL nuclei were further found to be functionally connected to the lateral visual network (Kumar et al., 2022), which is involved in motion and shape perception (Smith et al., 2009). Here, despite being known as first-order nuclei, we speculate that ventral thalamic regions may serve higher-order, integrative functions within visual processing, as it was described that first-order nuclei can also form a hub for interactions with multiple functional networks (Hwang et al., 2017).

MD nuclei have extensive connections with the prefrontal cortex (Haber & Mcfarland, 2001) and are primarily involved in executive cognitive function (Parnaudeau et al., 2017). For patients with psychotic disorders, MD nuclei were functionally hypoconnected with prefrontal areas (Avram et al., 2018; Woodward & Heckers, 2016) while being hyperconnected with sensorimotor areas (Anticevic, Cole, et al., 2014). Further, in a healthy population, MD nuclei were activated during perception of fused versus non-fused color (indicative of hallucinatory perception; Seo et al., 2022). Ventral and MD nuclei were also highlighted in recent reviews of relevant thalamic regions

contributing to drug- and pathology-related hallucinatory phenomena (Avram et al., 2021; Doss et al., 2021).

Together, these thalamic regions (AV, ventral, MD) show a similar thalamocortical hyperconnectivity pattern with visual cortices as recently reported in patients with chronic schizophrenia (Rolls et al., 2021), suggesting that the observed hyperconnectivity could be associated with hallucinatory experiences. However, the sparsity of literature linking these thalamic regions to the visual system makes it difficult to infer how exactly they contribute mechanistically to the emergence of visual hallucinations. This calls for further research into the functional involvement of higher-order nuclei in visual processing and consequently in hallucinatory experiences.

The role of higher-order thalamic nuclei in the formation of visual hallucinations may lie in their ability to orchestrate brain-wide cortical activity. AV, ventral, and MD nuclei all display strong connector hub properties for cortical functional networks (Hwang et al., 2017), which suggests that these thalamic areas are not only functionally specific, but also contribute to domain-general, brain-wide function (Shine et al., 2023). For example, cross-frequency coupling (CFC) may be a mechanism underlying FLS-induced effects, whereby the thalamus and/or EVC are entrained to alpha frequency, which consequently modulates large-scale cortical excitability occurring in the gamma frequency range (Canolty & Knight, 2010; Klimesch et al., 2007; Kosciessa et al., 2021; Wang et al., 2012). Given the importance of the thalamus in coordinating brain-wide activity, thalamocortical pathways have become a central feature of multiple theories of consciousness (Alkire et al., 2008; Aru et al., 2019; Purpura & Schiff, 1997; Tononi & Edelman, 1998; Ward, 2011), for example, the Dynamic Core Theory ((Tononi & Edelman, 1998); from which the Integrated Information Theory developed (Tononi, 2011; Tononi et al., 2016)), where subjective experiences might partly depend on orchestrating roles of thalamocortical interactions. Further, the Dendritic Integration Theory proposes that cortical layer 5p neurons, where dendritic signaling is under control of thalamocortical projections of higher-order nuclei, are critical for conscious experience (Aru et al., 2019). While our study does not directly address the neural mechanisms of conscious processing, it adds to an understanding regarding the role of thalamocortical interactions within visual experiences in the context of hallucinatory perception. Future research should continue to integrate how thalamocortical interactions contribute to conscious awareness and phenomenal characteristics of subjective experience.

4.4. Connectivity within visual areas

When exploring connectivity changes within the visual system, we found a consistent pattern of connectivity changes for 3 Hz and 10 Hz FLS. There was hyperconnectivity within two groups: (1) within EVC and (2) between upstream visual areas (e.g., LO2) and the IPS, while these two groups were decoupled from each other. Such altered corticocortical connectivity may have been mediated by the thalamus, which can sustain and modulate corticocortical functional connectivity (Schmitt et al., 2017). There are mixed findings of altered connectivity in the visual system during hallucinatory experiences following pharmacological intervention. Some studies found that LSD induced hypoconnectivity within EVC and within lateral visual regions (e.g., hV4/hMT) (Carhart-Harris et al., 2016; Müller et al., 2018), while a functional connectivity analysis found little effect on visual cortical connectivity (Bedford et al., 2023). Within our study, FLS-induced EVC hyperconnectivity likely reflects the visual sensory inputs that drive the consequent hallucinatory effects, while hallucinatory effects of LSD are mediated by serotonergic agonism and thus do not depend on EVC excitation (Aghajanian & Marek, 1999). Additionally, when using rDCM, LSD was shown to induce hypoconnectivity within visual regions while also increasing self-inhibitory connections exclusively amongst these areas (Bedford et al., 2023). Noting this, it can be speculated that FLS-driven excitatory input to the retina and EVC demands that upstream visual neurons increase their self-inhibitory modulations to avoid over-excitation of the system, which could lead to a decoupling between EVC and upstream areas. Moreover, it was recently shown that alpha entrainment through periodic visual flicker is associated with increased functional connectivity across occipitoparietal areas (Jaeger et al., 2023), suggesting that entrainment may underlie the hyperconnectivity between upstream visual areas and IPS reported here. However, similar corticocortical connectivity patterns for 3 Hz and 10 Hz FLS make it unlikely that alpha entrainment is critical for generating the observed connectivity patterns. Furthermore, similar corticocortical connectivity for both flicker frequencies suggests it may not correspond directly to the visual experience. Further research should explore in detail whether there is a phenomenal correlate of altered connectivity along the visual hierarchy in order to better understand the functional relevance of FLS-induced corticocortical connectivity changes.

5. LIMITATIONS AND FUTURE DIRECTIONS

It must be acknowledged that not all thalamic nuclei are accounted for in the AAL3 atlas. Particularly, the thalamic reticular nucleus, which forms a thin sheet surrounding the thalamus (Pinault, 2004), is known to exert inhibitory control on other thalamic nuclei, such as the LGN (Halassa & Sherman, 2019). Therefore, it is possible that changes in connectivity with thalamic regions may have been mediated by thalamic reticular activity. While future work could utilize other atlas parcellations of the thalamus that include reticular nuclei (e.g., thalamic probabilistic atlas (Iglesias et al., 2018)), Rolls et al. purposely omitted this ROI from their atlas due to its difficult structure for automated parcellation (Rolls et al., 2020). Accurate parcellation of the reticular nuclei may only be possible with a higher field MRI scanner (i.e., 7 T) and thus higher resolution images.

Moreover, with the quantification of functional connectivity, interpreting the directionality of effects is highly limited. The well-described anatomy of retinal inputs to the thalamus allows to draw some inference on feedforward signaling from the LGN to the cortex. Furthermore, the lack of direct retinal inputs to higher-order nuclei suggests that these are most likely driven by corticothalamic signaling. However, an interpretation of directionality beyond these is speculative. Future investigations could employ effective connectivity analyses, such as rDCM (Frässle et al., 2017, 2021), which can estimate directed connectivity strength within nodes of a whole-brain network. Thus, analyses such as rDCM could give more mechanistic insights into the sources of connectivity changes across thalamocortical and corticocortical loops. Furthermore, whole-brain analyses could identify other key changes in connectivity induced by FLS across the brain. For example, connectivity changes with the Default Mode Network are induced by various psychedelics drugs (see Gattuso et al., 2022, for review) and may be associated with other altered state phenomena that were shown to be affected by FLS, such as out-of-body sensations. Subsequent research in this direction would allow a more complete picture of how FLS influences subjective altered state experiences and the corresponding underlying connectivity patterns.

Finally, periodic visual stimuli have been reported to induce long-term potentiation (LTP) in visual cortices (Clapp et al., 2012), likely arising from interactions with LGN (Heynen & Bear, 2001; Sumner et al., 2021), which may drive the observed increase in thalamocortical connectivity. Future research can confirm whether FLS can reliably induce LTP in visual cortices, potentially unveiling its use in identifying LTP deficits in neuropsychiatric clinical populations.

6. CONCLUSIONS

Overall, we show that FLS induces thalamocortical hyperconnectivity between LGN, EVC, and proximal upstream areas of ventral and dorsal visual streams (i.e., hV4, VO1, V3a). Additionally, while only weak effects were found for the pulvinar, hyperconnectivity between other thalamic nuclei and visual areas was more apparent, that is, anterior, ventral, and mediodorsal nuclei. The hyperconnectivity between higher-order thalamic nuclei and upstream visual areas was only evident for 10 Hz FLS, which follows the parametric modulation of flicker frequency on subjective ratings of seeing patterns and colors. This suggests that, although thalamocortical hyperconnectivity with LGN may initially drive the FLS-induced effects, the subsequent cortical interactions with higher-order thalamic nuclei may be more relevant for the emergence of visual hallucinations. In sum, we identify, for the first time, the specific thalamic nuclei and visual areas that display altered connectivity during flicker-induced hallucinatory phenomena.

DATA AND CODE AVAILABILITY

The data that support the findings of this study are available on request to Ioanna A. Amaya (Ioanna.amaya@charite.de). Raw MRI data cannot be shared due to data protection. The code for MRI preprocessing and generating connectivity matrices is available at: https://github.com/ioannaamaya/FLS-rsfMRI.git.

AUTHOR CONTRIBUTIONS

Ioanna A. Amaya: Formal analysis, Data curation, Methodology, Visualization, and Writing—original draft. Marianna E. Schmidt: Data curation, Software. Marie T. Bartossek: Data curation. Johanna Kemmerer: Investigation, Data curation, and Methodology. Evgeniya Kirilina: Methodology, Resources. Till Nierhaus: Methodology, Formal analysis, Software, Supervision, and Writing—review & editing. Timo T. Schmidt: Conceptualization, Investigation, Project administration, Resources, Methodology, Software, Supervision, Visualization, Writing—original draft, and Writing—review & editing.

FUNDING

No external funding was received for the execution of this investigation. Ioanna A. Amaya is a PhD fellow of the Einstein Center for Neurosciences funded by Charité—Universitätsmedizin Berlin.

DECLARATION OF COMPETING INTEREST

None.

ACKNOWLEDGMENTS

We thank Light Attendance GmbH (Innsbruck, Austria) for generously providing a Lucia N°03 system free of charge. Marianna E. Schmidt is a PhD candidate of the Max Planck School of Cognition supported by the Federal Ministry of Education and Research (BMBF) and the Max Planck Society (MPG). We also acknowledge support by the Open Access Publication Fund of the Freie Universität Berlin.

SUPPLEMENTARY MATERIALS

Supplementary material for this article is available with the online version here: https://doi.org/10.1162/imag_a_00033.

REFERENCES

Adams, M. M., Hof, P. R., Gattass, R., Webster, M. J., & Ungerleider, L. G. (2000). Visual cortical projections and chemoarchitecture of macaque monkey pulvinar. *J Comp Neurol*, *419*, 377–393. https://doi.org/10.1002/(sici)1096-9861(20000410)419:3<377::aid-cne9>3.0.co;2-e

Adrian, E. D., & Matthews, B. H. C. (1934). The Berger rhythm: Potential changes from the occipital lobes in man. *Brain*, *57*, 355–385. https://doi.org/10.1093/brain/57.4.355

Aghajanian, G., & Marek, G. (1999). Serotonin and hallucinogens. *Neuropsychopharmacology*, *21*, 16–23. https://doi.org/10.1016/s0893-133x(98)00135-3

Alkire, M. T., Hudetz, A. G., & Tononi, G. (2008). Consciousness and anesthesia. *Science*, *322*, 876–880. https://doi.org/10.1126/science.1149213

Allefeld, C., Pütz, P., Kastner, K., & Wackermann, J. (2011). Flicker-light induced visual phenomena: Frequency dependence and specificity of whole percepts and percept features. *Conscious Cogn*, *20*, 1344–1362. https://doi.org/10.1016/j.concog.2010.10.026

Amaya, I. A., Behrens, N., Schwartzman, D. J., Hewitt, T., & Schmidt, T. T. (2023). Effect of frequency and rhythmicity on flicker light-induced hallucinatory phenomena. *PLoS One*, *18*, e0284271. https://doi.org/10.1371/journal.pone.0284271

Andolina, I. M., Jones, H. E., Wang, W., & Sillito, A. M. (2007). Corticothalamic feedback enhances stimulus response precision in the visual system. *Proc Natl Acad Sci*, *104*, 1685–1690. https://doi.org/10.1073/pnas.0609318104

Anticevic, A., Cole, M. W., Repovs, G., Murray, J. D., Brumbaugh, M. S., Winkler, A. M., Savic, A., Krystal, J. H., Pearlson, G. D., & Glahn, D. C. (2014). Characterizing thalamo-cortical disturbances in schizophrenia and bipolar illness. *Cereb Cortex*, *24*, 3116–3130. https://doi.org/10.1093/cercor/bht165

Anticevic, A., Yang, G., Savic, A., Murray, J. D., Cole, M. W., Repovs, G., Pearlson, G. D., & Glahn, D. C. (2014). Mediodorsal and visual thalamic connectivity differ in schizophrenia and bipolar disorder with and without psychosis history. *Schizophr Bull*, *40*, 1227–1243. https://doi.org/10.1093/schbul/sbu100

Aru, J., Suzuki, M., Rutiku, R., Larkum, M. E., & Bachmann, T. (2019). Coupling the state and contents of consciousness. *Front Syst Neurosci*, *13*, 43. https://doi.org/10.3389/fnsys.2019.00043

Ashburner, J., & Friston, K. J. (2005). Unified segmentation. *NeuroImage*, *26*, 839–851. https://doi.org/10.1016/j.neuroimage.2005.02.018

Avram, M., Brandl, F., Bäuml, J., & Sorg, C. (2018). Cortico-thalamic hypo- and hyperconnectivity extend consistently to basal ganglia in schizophrenia. *Neuropsychopharmacology*, *43*, 1–10. https://doi.org/10.1038/s41386-018-0059-z

Avram, M., Müller, F., Rogg, H., Korda, A., Andreou, C., Holze, F., Vizeli, P., Ley, L., Liechti, M. E., & Borgwardt, S. (2022). Characterizing thalamocortical (Dys) connectivity following D-amphetamine, LSD, and MDMA administration. *Biol Psychiatry Cogn Neurosci Neuroimaging*, *7*, 885–894. https://doi.org/10.1016/j.bpsc.2022.04.003

Avram, M., Rogg, H., Korda, A., Andreou, C., Müller, F., & Borgwardt, S. (2021). Bridging the gap? Altered thalamocortical connectivity in psychotic and psychedelic states. *Front Psychiatry*, *12*, 706017. https://doi.org/10.3389/fpsyt.2021.706017

Bartossek, M. T., Kemmerer, J., & Schmidt, T. T. (2021). Altered states phenomena induced by visual flicker light stimulation. *PLoS One*, *16*, e0253779. https://doi.org/10.1371/journal.pone.0253779

Bedford, P., Hauke, D. J., Wang, Z., Roth, V., Nagy-Huber, M., Holze, F., Ley, L., Vizeli, P., Liechti, M. E., Borgwardt, S., Müller, F., & Diaconescu, A. O. (2023). The effect of lysergic acid diethylamide (LSD) on whole-brain functional and effective connectivity. *Neuropsychopharmacology*, *48*, 1175–1183. https://doi.org/10.1038/s41386-023-01574-8

Behzadi, Y., Restom, K., Liau, J., & Liu, T. T. (2007). A component based noise correction method (CompCor) for BOLD and perfusion based fMRI. *NeuroImage*, *37*, 90–101. https://doi.org/10.1016/j.neuroimage.2007.04.042

Benevento, L. A., & Rezak, M. (1976). The cortical projections of the inferior pulvinar and adjacent lateral pulvinar in the rhesus monkey (*Macaca mulatta*): An autoradiographic study. *Brain Res*, *108*, 1–24. https://doi.org/10.1016/0006-8993(76)90160-8

Bolay, H. (2020). Thalamocortical network interruption: A fresh view for migraine symptoms. *Turk J Med Sci*, *50*, 1651–1654. https://doi.org/10.3906/sag-2005-21

Botzung, A., Denkova, E., & Manning, L. (2008). Experiencing past and future personal events: Functional neuroimaging evidence on the neural bases of mental

time travel. *Brain Cogn*, *66*, 202–212. https://doi.org/10.1016/j.bandc.2007.07.011
Briggs, F. (2020). Role of feedback connections in central visual processing. *Annu Rev Vis Sci*, *6*, 1–22. https://doi.org/10.1146/annurev-vision-121219-081716
Budd, J. M. L. (2004). How much feedback from visual cortex to lateral geniculate nucleus in cat: A perspective. *Vis Neurosci*, *21*, 487–500. https://doi.org/10.1017/s0952523804214018
Butler, T. C., Benayoun, M., Wallace, E., Drongelen, W. van, Goldenfeld, N., & Cowan, J. (2012). Evolutionary constraints on visual cortex architecture from the dynamics of hallucinations. *Proc Natl Acad Sci*, *109*, 606–609. https://doi.org/10.1073/pnas.1118672109
Byne, W., Buchsbaum, M. S., Mattiace, L. A., Hazlett, E. A., Kemether, E., Elhakem, S. L., Purohit, D. P., Haroutunian, V., & Jones, L. (2002). Postmortem assessment of thalamic nuclear volumes in subjects with schizophrenia. *Am J Psychiatry*, *159*, 59–65. https://doi.org/10.1176/appi.ajp.159.1.59
Canolty, R. T., & Knight, R. T. (2010). The functional role of cross-frequency coupling. *Trends Cogn Sci*, *14*, 506–515. https://doi.org/10.1016/j.tics.2010.09.001
Carhart-Harris, R. L., Erritzoe, D., Williams, T., Stone, J. M., Reed, L. J., Colasanti, A., Tyacke, R. J., Leech, R., Malizia, A. L., Murphy, K., Hobden, P., Evans, J., Feilding, A., Wise, R. G., & Nutt, D. J. (2012). Neural correlates of the psychedelic state as determined by fMRI studies with psilocybin. *Proc Natl Acad Sci*, *109*, 2138–2143. https://doi.org/10.1073/pnas.1119598109
Carhart-Harris, R. L., Muthukumaraswamy, S., Roseman, L., Kaelen, M., Droog, W., Murphy, K., Tagliazucchi, E., Schenberg, E. E., Nest, T., Orban, C., Leech, R., Williams, L. T., Williams, T. M., Bolstridge, M., Sessa, B., McGonigle, J., Sereno, M. I., Nichols, D., Hellyer, P. J., … Nutt, D. J. (2016). Neural correlates of the LSD experience revealed by multimodal neuroimaging. *Proc Natl Acad Sci*, *113*, 4853–4858. https://doi.org/10.1073/pnas.1518377113
Chen, Y., Fallon, N., Kreilkamp, B. A. K., Denby, C., Bracewell, M., Das, K., Pegg, E., Mohanraj, R., Marson, A. G., & Keller, S. S. (2021). Probabilistic mapping of thalamic nuclei and thalamocortical functional connectivity in idiopathic generalised epilepsy. *Hum Brain Mapp*, *42*, 5648–5664. https://doi.org/10.1002/hbm.25644
Clapp, W. C., Hamm, J. P., Kirk, I. J., & Teyler, T. J. (2012). Translating long-term potentiation from animals to humans: a novel method for noninvasive assessment of cortical plasticity. *Biol Psychiatry*, *71*, 496–502. https://doi.org/10.1016/j.biopsych.2011.08.021
Cowan, J. D. (2013). Visual hallucinations and migraine aura. In *Encyclopedia of Computational Neuroscience* (pp. 1–11). Springer. https://doi.org/10.1007/978-1-4614-7320-6_515-1
Danos, P., Baumann, B., Bernstein, H.-G., Franz, M., Stauch, R., Northoff, G., Krell, D., Falkai, P., & Bogerts, B. (1998). Schizophrenia and anteroventral thalamic nucleus: Selective decrease of parvalbumin-immunoreactive thalamocortical projection neurons. *Psychiatry Res Neuroimaging*, *82*, 1–10. https://doi.org/10.1016/s0925-4927(97)00071-1
Danos, P., Baumann, B., Krämer, A., Bernstein, H.-G., Stauch, R., Krell, D., Falkai, P., & Bogerts, B. (2003). Volumes of association thalamic nuclei in schizophrenia: A postmortem study. *Schizophr Res*, *60*, 141–155. https://doi.org/10.1016/s0920-9964(02)00307-9
D'Argembeau, A., Xue, G., Lu, Z.-L., Linden, M. V. der, & Bechara, A. (2008). Neural correlates of envisioning emotional events in the near and far future. *NeuroImage*, *40*, 398–407. https://doi.org/10.1016/j.neuroimage.2007.11.025
Dittrich, A. (1998). The standardized psychometric assessment of altered states of consciousness (ASCs) in humans. *Pharmacopsychiatry*, *31*, 80–84. https://doi.org/10.1055/s-2007-979351
Doss, M. K., Madden, M. B., Gaddis, A., Nebel, M. B., Griffiths, R. R., Mathur, B. N., & Barrett, F. S. (2021). Models of psychedelic drug action: Modulation of cortical-subcortical circuits. *Brain*, *145*, 441–456. https://doi.org/10.1093/brain/awab406
Engel, S. A., Glover, G. H., & Wandell, B. A. (1997). Retinotopic organization in human visual cortex and the spatial precision of functional MRI. *Cereb Cortex*, *7*, 181–192. https://doi.org/10.1093/cercor/7.2.181
Erskine, D., Thomas, A. J., Attems, J., Taylor, J., McKeith, I. G., Morris, C. M., & Khundakar, A. A. (2017). Specific patterns of neuronal loss in the pulvinar nucleus in dementia with lewy bodies. *Mov Disord*, *32*, 414–422. https://doi.org/10.1002/mds.26887
Ffytche, D. H. (2005). Visual hallucinations and the Charles Bonnet syndrome. *Curr Psychiatry Rep*, *7*, 168–179. https://doi.org/10.1007/s11920-005-0050-3
Ffytche, D. H. (2008). The hodology of hallucinations. *Cortex*, *44*, 1067–1083. https://doi.org/10.1016/j.cortex.2008.04.005
Frässle, S., Harrison, S. J., Heinzle, J., Clementz, B. A., Tamminga, C. A., Sweeney, J. A., Gershon, E. S., Keshavan, M. S., Pearlson, G. D., Powers, A., & Stephan, K. E. (2021). Regression dynamic causal modeling for resting-state fMRI. *Hum Brain Mapp*, *42*, 2159–2180. https://doi.org/10.1002/hbm.25357
Frässle, S., Lomakina, E. I., Razi, A., Friston, K. J., Buhmann, J. M., & Stephan, K. E. (2017). Regression DCM for fMRI. *NeuroImage*, *155*, 406–421. https://doi.org/10.1016/j.neuroimage.2017.02.090
Gattass, R., Galkin, T. W., Desimone, R., & Ungerleider, L. G. (2014). Subcortical connections of area V4 in the macaque. *J Comp Neurol*, *522*, 1941–1965. https://doi.org/10.1002/cne.23513
Gattass, R., Soares, J. G. M., & Lima, B. (2017). The pulvinar thalamic nucleus of non-human primates: Architectonic and functional subdivisions. In *Advances in Anatomy, Embryology and Cell Biology* (Vol. *225*, pp. 57–60). https://doi.org/10.1007/978-3-319-70046-5_12
Gattuso, J. J., Perkins, D., Ruffell, S., Lawrence, A. J., Hoyer, D., Jacobson, L. H., Timmermann, C., Castle, D., Rossell, S. L., Downey, L. A., Pagni, B. A., Galvão-Coelho, N. L., Nutt, D., & Sarris, J. (2022). Default mode network modulation by psychedelics: A systematic review. *Int J Neuropsychopharmacol*, *26*, 155–188. https://doi.org/10.1093/ijnp/pyac074
Geyer, M. A., & Vollenweider, F. X. (2008). Serotonin research: Contributions to understanding psychoses. *Trends Pharmacol Sci*, *29*, 445–453. https://doi.org/10.1016/j.tips.2008.06.006
Grill-Spector, K., Kushnir, T., Hendler, T., Edelman, S., Itzchak, Y., & Malach, R. (1998). A sequence of object-processing stages revealed by fMRI in the human

occipital lobe. *Hum Brain Mapp*, *6*, 316–328. https://pubmed.ncbi.nlm.nih.gov/9704268/
Guedj, C., & Vuilleumier, P. (2020). Functional connectivity fingerprints of the human pulvinar: Decoding its role in cognition. *NeuroImage*, *221*, 117162. https://doi.org/10.1016/j.neuroimage.2020.117162
Haber, S., & Mcfarland, N. R. (2001). The place of the thalamus in frontal cortical-basal ganglia circuits. *Neuroscientist*, *7*, 315–324. https://doi.org/10.1177/107385840100700408
Hádinger, N., Bősz, E., Tóth, B., Vantomme, G., Lüthi, A., & Acsády, L. (2023). Region-selective control of the thalamic reticular nucleus via cortical layer 5 pyramidal cells. *Nat Neurosci*, *26*, 116–130. https://doi.org/10.1038/s41593-022-01217-z
Halassa, M. M., & Sherman, S. M. (2019). Thalamocortical circuit motifs: A general framework. *Neuron*, *103*, 762–770. https://doi.org/10.1016/j.neuron.2019.06.005
Hassabis, D., Kumaran, D., & Maguire, E. A. (2007). Using imagination to understand the neural basis of episodic memory. *J Neurosci*, *27*, 14365–14374. https://doi.org/10.1523/jneurosci.4549-07.2007
Heynen, A. J., & Bear, M. F. (2001). Long-term potentiation of thalamocortical transmission in the adult visual cortex in vivo. *J Neurosci*, *21*, 9801–9813. https://doi.org/10.1523/jneurosci.21-24-09801.2001
Hirschfeld, T., Prugger, J., Majić, T., & Schmidt, T. T. (2023). Dose-response relationships of LSD-induced subjective experiences in humans. *Neuropsychopharmacology*, *48*, 1602–1611. https://doi.org/10.1038/s41386-023-01588-2
Hirschfeld, T., & Schmidt, T. T. (2021). Dose–response relationships of psilocybin-induced subjective experiences in humans. *J Psychopharmacol*, *35*, 384–397. https://doi.org/10.1177/0269881121992676
Hwang, K., Bertolero, M. A., Liu, W. B., & D'Esposito, M. (2017). The human thalamus is an integrative hub for functional brain networks. *J Neurosci*, *37*, 5594–5607. https://doi.org/10.1523/jneurosci.0067-17.2017
Iglehart, C., Monti, M., Cain, J., Tourdias, T., & Saranathan, M. (2020). A systematic comparison of structural-, structural connectivity-, and functional connectivity-based thalamus parcellation techniques. *Brain Struct Funct*, *225*, 1631–1642. https://doi.org/10.1007/s00429-020-02085-8
Iglesias, J. E., Insausti, R., Lerma-Usabiaga, G., Bocchetta, M., Leemput, K. V., Greve, D. N., Kouwe, A. van der, Initiative, the A. D. N., Fischl, B., Caballero-Gaudes, C., & Paz-Alonso, P. M. (2018). A probabilistic atlas of the human thalamic nuclei combining ex vivo MRI and histology. *NeuroImage*, *183*, 314–326. https://doi.org/10.1016/j.neuroimage.2018.08.012
Jaeger, C., Nuttall, R., Zimmermann, J., Dowsett, J., Preibisch, C., Sorg, C., & Wohlschlaeger, A. (2023). Targeted rhythmic visual stimulation at individual participants' intrinsic alpha frequency causes selective increase of occipitoparietal BOLD-fMRI and EEG functional connectivity. *NeuroImage*, *270*, 119981. https://doi.org/10.1016/j.neuroimage.2023.119981
Jan, T., & Castillo, J. Del. (2012). Visual hallucinations: Charles Bonnet syndrome. *West J Emerg Med*, *13*, 544–547. https://doi.org/10.5811/westjem.2012.7.12891
Johansen-Berg, H., Behrens, T. E. J., Sillery, E., Ciccarelli, O., Thompson, A. J., Smith, S. M., & Matthews, P. M. (2005). Functional–anatomical validation and individual variation of diffusion tractography-based segmentation of the human thalamus. *Cereb Cortex*, *15*, 31–39. https://doi.org/10.1093/cercor/bhh105
Kaas, J. H., & Lyon, D. C. (2007). Pulvinar contributions to the dorsal and ventral streams of visual processing in primates. *Brain Res Rev*, *55*, 285–296. https://doi.org/10.1016/j.brainresrev.2007.02.008
Kim, J. B., Suh, S., Seo, W., Oh, K., Koh, S., & Kim, J. H. (2014). Altered thalamocortical functional connectivity in idiopathic generalized epilepsy. *Epilepsia*, *55*, 592–600. https://doi.org/10.1111/epi.12580
Klimesch, W., Sauseng, P., & Hanslmayr, S. (2007). EEG alpha oscillations: The inhibition–timing hypothesis. *Brain Res Rev*, *53*, 63–88. https://doi.org/10.1016/j.brainresrev.2006.06.003
Klüver, H. (1966). *Mescal and Mechanisms of Hallucinations.* University of Chicago Press. https://www.google.de/books/edition/Mescal_and_Mechanisms_of_Hallucinations/LnKpbwAACAAJ?hl=en
Kosciessa, J. Q., Lindenberger, U., & Garrett, D. D. (2021). Thalamocortical excitability modulation guides human perception under uncertainty. *Nat Commun*, *12*, 2430. https://doi.org/10.1038/s41467-021-22511-7
Kumar, V. J., Beckmann, C. F., Scheffler, K., & Grodd, W. (2022). Relay and higher-order thalamic nuclei show an intertwined functional association with cortical-networks. *Commun Biol*, *5*, 1187. https://doi.org/10.1038/s42003-022-04126-w
Lawrence, D. W., Carhart-Harris, R., Griffiths, R., & Timmermann, C. (2022). Phenomenology and content of the inhaled N, N-dimethyltryptamine (N, N-DMT) experience. *Sci Rep*, *12*, 8562. https://doi.org/10.1038/s41598-022-11999-8
Lieslehto, J., Jääskeläinen, E., Kiviniemi, V., Haapea, M., Jones, P. B., Murray, G. K., Veijola, J., Dannlowski, U., Grotegerd, D., Meinert, S., Hahn, T., Ruef, A., Isohanni, M., Falkai, P., Miettunen, J., Dwyer, D. B., & Koutsouleris, N. (2021). The progression of disorder-specific brain pattern expression in schizophrenia over 9 years. *NPJ Schizophr*, *7*, 32. https://doi.org/10.1038/s41537-021-00157-0
Lomi, E., Jeffery, K. J., & Mitchell, A. S. (2023). Convergence of direction, location and theta in the rat anteroventral thalamic nucleus. *bioRxiv*, 2023.01.11.523585. https://doi.org/10.1101/2023.01.11.523585
Malach, R., Reppas, J. B., Benson, R. R., Kwong, K. K., Jiang, H., Kennedy, W. A., Ledden, P. J., Brady, T. J., Rosen, B. R., & Tootell, R. B. (1995). Object-related activity revealed by functional magnetic resonance imaging in human occipital cortex. *Proc Natl Acad Sci*, *92*, 8135–8139. https://doi.org/10.1073/pnas.92.18.8135
Martinelli, D., Castellazzi, G., Icco, R. D., Bacila, A., Allena, M., Faggioli, A., Sances, G., Pichiecchio, A., Borsook, D., Wheeler-Kingshott, C. A. M. G., & Tassorelli, C. (2021). Thalamocortical connectivity in experimentally-induced migraine attacks: A pilot study. *Brain Sci*, *11*, 165. https://doi.org/10.3390/brainsci11020165
Mathewson, K. E., Prudhomme, C., Fabiani, M., Beck, D. M., Lleras, A., & Gratton, G. (2012). Making waves in the stream of consciousness: Entraining oscillations in EEG alpha and fluctuations in visual awareness with rhythmic visual stimulation. *J Cogn Neurosci*, *24*, 2321–2333. https://doi.org/10.1162/jocn_a_00288

Montgomery, C., Amaya, I. A., & Schmidt, T. T. (2023). Flicker light stimulation enhances the emotional response to music: A comparison study to the effects of psychedelics. *PsyArXiv*. https://doi.org/10.31234/osf.io/s6dnr

Müller, F., Dolder, P. C., Schmidt, A., Liechti, M. E., & Borgwardt, S. (2018). Altered network hub connectivity after acute LSD administration. *Neuroimage Clin*, *18*, 694–701. https://doi.org/10.1016/j.nicl.2018.03.005

Müller, F., Lenz, C., Dolder, P., Lang, U., Schmidt, A., Liechti, M., & Borgwardt, S. (2017). Increased thalamic resting-state connectivity as a core driver of LSD-induced hallucinations. *Acta Psychiat Scand*, *136*, 648–657. https://doi.org/10.1111/acps.12818

Murphy, K., & Fox, M. D. (2017). Towards a consensus regarding global signal regression for resting state functional connectivity MRI. *NeuroImage*, *154*, 169–173. https://doi.org/10.1016/j.neuroimage.2016.11.052

Murphy, P. C., Duckett, S. G., & Sillito, A. M. (1999). Feedback connections to the lateral geniculate nucleus and cortical response properties. *Science*, *286*, 1552–1554. https://doi.org/10.1126/science.286.5444.1552

Notbohm, A., & Herrmann, C. S. (2016). Flicker regularity is crucial for entrainment of alpha oscillations. *Front Hum Neurosci*, *10*, 503. https://doi.org/10.3389/fnhum.2016.00503

Notbohm, A., Kurths, J., & Herrmann, C. S. (2016). Modification of brain oscillations via rhythmic light stimulation provides evidence for entrainment but not for superposition of event-related responses. *Front Hum Neurosci*, *10*, 10. https://doi.org/10.3389/fnhum.2016.00010

Oldfield, R. C. (1971). The assessment and analysis of handedness: The Edinburgh inventory. *Neuropsychologia*, *9*, 97–113. https://doi.org/10.1016/0028-3932(71)90067-4

Panayiotopoulos, C. P. (1994). Elementary visual hallucinations in migraine and epilepsy. *J Neurol Neurosurg Psychiatry*, *57*, 1371. https://doi.org/10.1136/jnnp.57.11.1371

Parnaudeau, S., Bolkan, S. S., & Kellendonk, C. (2017). The mediodorsal thalamus: An essential partner of the prefrontal cortex for cognition. *Biol Psychiatry*, *83*, 648–656. https://doi.org/10.1016/j.biopsych.2017.11.008

Pearson, J., Chiou, R., Rogers, S., Wicken, M., Heitmann, S., & Ermentrout, B. (2016). Sensory dynamics of visual hallucinations in the normal population. *eLife*, *5*, e17072. https://doi.org/10.7554/elife.17072

Percheron, G., François, C., Talbi, B., Yelnik, J., & Fénelon, G. (1996). The primate motor thalamus. *Brain Res Brain Res Rev*, *22*, 93–181. https://pubmed.ncbi.nlm.nih.gov/8883918/

Persichetti, A. S., Thompson-Schill, S. L., Butt, O. H., Brainard, D. H., & Aguirre, G. K. (2015). Functional magnetic resonance imaging adaptation reveals a noncategorical representation of hue in early visual cortex. *J Vis*, *15*, 18. https://doi.org/10.1167/15.6.18

Peyrache, A., Duszkiewicz, A. J., Viejo, G., & Angeles-Duran, S. (2019). Thalamocortical processing of the head-direction sense. *Prog Neurobiol*, *183*, 101693. https://doi.org/10.1016/j.pneurobio.2019.101693

Pinault, D. (2004). The thalamic reticular nucleus: Structure, function and concept. *Brain Res Rev*, *46*, 1–31. https://doi.org/10.1016/j.brainresrev.2004.04.008

Power, J. D., Barnes, K. A., Snyder, A. Z., Schlaggar, B. L., & Petersen, S. E. (2012). Spurious but systematic correlations in functional connectivity MRI networks arise from subject motion. *NeuroImage*, *59*, 2142–2154. https://doi.org/10.1016/j.neuroimage.2011.10.018

Preller, K. H., Razi, A., Zeidman, P., Stämpfli, P., Friston, K. J., & Vollenweider, F. X. (2019). Effective connectivity changes in LSD-induced altered states of consciousness in humans. *Proc Natl Acad Sci*, *116*, 2743–2748. https://doi.org/10.1073/pnas.1815129116

Prugger, J., Derdiyok, E., Dinkelacker, J., Costines, C., & Schmidt, T. T. (2022). The Altered States Database: Psychometric data from a systematic literature review. *Sci Data*, *9*, 720. https://doi.org/10.1038/s41597-022-01822-4

Purpura, K. P., & Schiff, N. D. (1997). The thalamic intralaminar nuclei: A role in visual awareness. *Neuroscientist*, *3*, 8–15. https://doi.org/10.1177/107385849700300110

Ramsay, I. S. (2019). An activation likelihood estimate meta-analysis of thalamocortical dysconnectivity in psychosis. *Biol Psychiatry Cogn Neurosci Neuroimaging*, *4*, 859–869. https://doi.org/10.1016/j.bpsc.2019.04.007

Reinhold, K., Resulaj, A., Scanziani, M. (2023). Brain State-Dependent Modulation of Thalamic Visual Processing by Cortico-Thalamic Feedback. *J Neurosci*, *43*, 1540–1554. https://doi.org/10.1523/jneurosci.2124-21.2022

Richards, W. (1971). The fortification illusions of migraines. *Sci Am*, *224*, 88–96. https://doi.org/10.1038/scientificamerican0571-88

Ro, T., Farnè, A., Johnson, R. M., Wedeen, V., Chu, Z., Wang, Z. J., Hunter, J. V., & Beauchamp, M. S. (2007). Feeling sounds after a thalamic lesion. *Ann Neurol*, *62*, 433–441. https://doi.org/10.1002/ana.21219

Rogers, S., Keogh, R., & Pearson, J. (2021). Hallucinations on demand: The utility of experimentally induced phenomena in hallucination research. *Philos Trans R Soc B*, *376*, 20200233. https://doi.org/10.1098/rstb.2020.0233

Rolls, E. T., Cheng, W., & Feng, J. (2021). Brain dynamics: The temporal variability of connectivity, and differences in schizophrenia and ADHD. *Transl Psychiatry*, *11*, 70. https://doi.org/10.1038/s41398-021-01197-x

Rolls, E. T., Huang, C.-C., Lin, C.-P., Feng, J., & Joliot, M. (2020). Automated anatomical labelling atlas 3. *NeuroImage*, *206*, 116189. https://doi.org/10.1016/j.neuroimage.2019.116189

Rovó, Z., Ulbert, I., & Acsády, L. (2012). Drivers of the primate thalamus. *J Neurosci*, *32*, 17894–17908. https://doi.org/10.1523/jneurosci.2815-12.2012

Roy, D. S., Zhang, Y., Aida, T., Shen, C., Skaggs, K. M., Hou, Y., Fleishman, M., Mosto, O., Weninger, A., & Feng, G. (2022). Anterior thalamic circuits crucial for working memory. *Proc Natl Acad Sci*, *119*, e2118712119. https://doi.org/10.1073/pnas.2118712119

Rule, M., Stoffregen, M., & Ermentrout, B. (2011). A model for the origin and properties of flicker-induced geometric phosphenes. *PLoS Comput Biol*, *7*, e1002158. https://doi.org/10.1371/journal.pcbi.1002158

Saalmann, Y. B., Pinsk, M. A., Wang, L., Li, X., & Kastner, S. (2012). The pulvinar regulates information transmission between cortical areas based on attention demands. *Science*, *337*, 753–756. https://doi.org/10.1126/science.1223082

Safari, V., Nategh, M., Dargahi, L., Zibaii, M. E., Khodagholi, F., Rafiei, S., Khatami, L., & Motamedi, F. (2020). Individual subnuclei of the rat anterior thalamic nuclei differently affect spatial memory and passive avoidance tasks. *Neuroscience*, *444*, 19–32. https://doi.org/10.1016/j.neuroscience.2020.07.046

Schmidt, T. T., Jagannathan, N., Ljubljanac, M., Xavier, A., & Nierhaus, T. (2020). The multimodal Ganzfeld-induced altered state of consciousness induces decreased thalamo-cortical coupling. *Sci Rep*, *10*, 18686. https://doi.org/10.1038/s41598-020-75019-3

Schmidt, T. T., & Majić, T. (2017). *Handbuch Psychoaktive Substanzen* (pp. 153–171). Springer. https://doi.org/10.1007/978-3-642-55125-3_65

Schmitt, L. I., Wimmer, R. D., Nakajima, M., Happ, M., Mofakham, S., & Halassa, M. M. (2017). Thalamic amplification of cortical connectivity sustains attentional control. *Nature*, *545*, 219–223. https://doi.org/10.1038/nature22073

Schneider, M., Tzanou, A., Uran, C., & Vinck, M. (2023). Cell-type-specific propagation of visual flicker. *Cell Rep*, *42*, 112492. https://doi.org/10.1016/j.celrep.2023.112492

Schott, G. D. (2007). Exploring the visual hallucinations of migraine aura: The tacit contribution of illustration. *Brain*, *130*, 1690–1703. https://doi.org/10.1093/brain/awl348

Schwartzman, D. J., Schartner, M., Ador, B. B., Simonelli, F., Chang, A. Y.-C., & Seth, A. K. (2019). Increased spontaneous EEG signal diversity during stroboscopically-induced altered states of consciousness. *bioRxiv*, 511766. https://doi.org/10.1101/511766

Seo, J., Kim, D.-J., Choi, S.-H., Kim, H., & Min, B.-K. (2022). The thalamocortical inhibitory network controls human conscious perception. *NeuroImage*, *264*, 119748. https://doi.org/10.1016/j.neuroimage.2022.119748

Sereno, M. I., Dale, A. M., Reppas, J. B., Kwong, K. K., Belliveau, J. W., Brady, T. J., Rosen, B. R., & Tootell, R. B. H. (1995). Borders of multiple visual areas in humans revealed by functional magnetic resonance imaging. *Science*, *268*, 889–893. https://doi.org/10.1126/science.7754376

Sharp, P. E., Blair, H. T., & Cho, J, (2001). The anatomical and computational basis of the rat head-direction cell signal. *Trends Neurosci*, *24*, 289–294. https://doi.org/10.1016/s0166-2236(00)01797-5

Sherman, S. M. (2016). Thalamus plays a central role in ongoing cortical functioning. *Nat Neurosci*, *19*, 533–541. https://doi.org/10.1038/nn.4269

Sherman, S. M., & Guillery, R. W. (2006). *Exploring the Thalamus and Its Role in Cortical Function*, 2nd ed. MIT Press. https://mitpress.mit.edu/9780262513449/exploring-the-thalamus-and-its-role-in-cortical-function

Shine, J. M., Lewis, L. D., Garrett, D. D., & Hwang, K. (2023). The impact of the human thalamus on brain-wide information processing. *Nat Rev Neurosci*, *24*, 416–430. https://doi.org/10.1038/s41583-023-00701-0

Shipp, S. (2003). The functional logic of corticopulvinar connections. *Philos Trans R Soc Lond B Biol Sci*, *358*, 1605–1624. https://doi.org/10.1098/rstb.2002.1213

Sillito, A. M., Jones, H. E., Gerstein, G. L., & West, D. C. (1994). Feature-linked synchronization of thalamic relay cell firing induced by feedback from the visual cortex. *Nature*, *369*, 479–482. https://doi.org/10.1038/369479a0

Silson, E. H., McKeefry, D. J., Rodgers, J., Gouws, A. D., Hymers, M., & Morland, A. B. (2013). Specialized and independent processing of orientation and shape in visual field maps LO1 and LO2. *Nat Neurosci*, *16*, 267–269. https://doi.org/10.1038/nn.3327

Smith, S. M., Fox, P. T., Miller, K. L., Glahn, D. C., Fox, P. M., Mackay, C. E., Filippini, N., Watkins, K. E., Toro, R., Laird, A. R., & Beckmann, C. F. (2009). Correspondence of the brain's functional architecture during activation and rest. *Proc Natl Acad Sci*, *106*, 13040–13045. https://doi.org/10.1073/pnas.0905267106

Soares, J. G. M., GATTASS, R., SOUZA, A. P. B., ROSA, M. G. P., FIORANI, M., & Brandão, B. L. (2001). Connectional and neurochemical subdivisions of the pulvinar in cebus monkeys. *Vis Neurosci*, *18*, 25–41. https://doi.org/10.1017/s0952523801181034

Sumner, R. L., Spriggs, M. J., & Shaw, A. D. (2021). Modelling thalamocortical circuitry shows that visually induced LTP changes laminar connectivity in human visual cortex. *PLoS Comput Biol*, *17*, e1008414. https://doi.org/10.1371/journal.pcbi.1008414

Szpunar, K. K., Watson, J. M., & McDermott, K. B. (2007). Neural substrates of envisioning the future. *Proc Natl Acad Sci*, *104*, 642–647. https://doi.org/10.1073/pnas.0610082104

Taube, J. S. (2007). The head direction signal: Origins and sensory-motor integration. *Annu Rev Neurosci*, *30*, 181–207. https://doi.org/10.1146/annurev.neuro.29.051605.112854

Tononi, G. (2011). Integrated information theory of consciousness: An updated account. *Arch Ital Biol*, *150*, 56–90. https://doi.org/10.4449/aib.v149i5.1388

Tononi, G., Boly, M., Massimini, M., & Koch, C. (2016). Integrated information theory: From consciousness to its physical substrate. *Nat Rev Neurosci*, *17*, 450–461. https://doi.org/10.1038/nrn.2016.44

Tononi, G., & Edelman, G. M. (1998). Consciousness and complexity. *Science*, *282*, 1846–1851. https://doi.org/10.1126/science.282.5395.1846

Tu, Y., Fu, Z., Zeng, F., Maleki, N., Lan, L., Li, Z., Park, J., Wilson, G., Gao, Y., Liu, M., Calhoun, V., Liang, F., & Kong, J. (2019). Abnormal thalamocortical network dynamics in migraine. *Neurology*, *92*, e2706–e2716. https://doi.org/10.1212/wnl.0000000000007607

Ungerleider, L. G., & Haxby, J. V. (1994). 'What' and 'where' in the human brain. *Curr Opin Neurobiol*, *4*, 157–165. https://doi.org/10.1016/0959-4388(94)90066-3

Vollenweider, F. X., & Geyer, M. A. (2001). A systems model of altered consciousness: Integrating natural and drug-induced psychoses. *Brain Res Bull*, *56*, 495–507. https://doi.org/10.1016/s0361-9230(01)00646-3

Vollenweider, F. X., & Preller, K. H. (2020). Psychedelic drugs: Neurobiology and potential for treatment of psychiatric disorders. *Nat Rev Neurosci*, *21*, 611–624. https://doi.org/10.1038/s41583-020-0367-2

Wang, L., Mruczek, R. E. B., Arcaro, M. J., & Kastner, S. (2015). Probabilistic maps of visual topography in human cortex. *Cereb Cortex*, *25*, 3911–3931. https://doi.org/10.1093/cercor/bhu277

Wang, L., Saalmann, Y. B., Pinsk, M. A., Arcaro, M. J., & Kastner, S. (2012). Electrophysiological low-frequency coherence and cross-frequency coupling contribute to BOLD connectivity. *Neuron*, *76*, 1010–1020. https://doi.org/10.1016/j.neuron.2012.09.033

Ward, L. M. (2011). The thalamic dynamic core theory of conscious experience. *Conscious Cogn*, *20*, 464–486. https://doi.org/10.1016/j.concog.2011.01.007

Wilkinson, F. (2004). Auras and other hallucinations: Windows on the visual brain. *Prog Brain Res*, *144*, 305–320. https://doi.org/10.1016/s0079-6123(03)14421-4

Woodward, N. D., & Heckers, S. (2016). Mapping thalamocortical functional connectivity in chronic and early stages of psychotic disorders. *Biol Psychiatry*, *79*, 1016–1025. https://doi.org/10.1016/j.biopsych.2015.06.026

Zeki, S., Watson, J., Lueck, C., Friston, K., Kennard, C., & Frackowiak, R. (1991). A direct demonstration of functional specialization in human visual cortex. *J Neurosci*, *11*, 641–649. https://doi.org/10.1523/jneurosci.11-03-00641.1991